Preparation and pharmacological study of *Cnidium monnieri* volatile oil cream

TINGTING SUN[1], LEYAO DANG[1], BINYUE ZHENG[1], XINGYU DANG[1], XINYU GOU[1], JIE WANG[1], JINHUI WANG[1], XIAOFEI ZHANG[1], JING SUN[1], YAJUN SHI[1], DONGYAN GUO[1], JUNBO ZOU[1], HENGLEI NIU[1], XIN SUI[2] and YING WANG[1]

[1]College of Pharmacy, Shaanxi University of Chinese Medicine, Xianyang, Shaanxi 712046, P.R. China; [2]Beijing Kailipesu Biotechnology Co., Ltd., Daxing, Beijing 102600, P.R. China

Received February 3, 2026; Accepted April 29, 2026

DOI: 10.3892/br.2026.2164

Abstract. Eczema, a chronic inflammatory skin condition, causes persistent discomfort and impairs patients' quality of life. *Cnidium monnieri* has been traditionally used for its anti-inflammatory and antipruritic properties. The present study aimed to develop an optimized formulation of *Cnidium monnieri* volatile oil cream (CMVOC) and evaluate its anti-inflammatory effects in an eczema model. A single-factor and response surface optimization approach was used to determine the optimal cream formulation. The formulation was evaluated based on appearance, physical stability, particle size and moisturizing capacity. An eczema model was induced using 2,4-dinitrochlorobenzene (DNCB) in mice. Serum levels of IL-6 and IL-17 were measured by ELISA, skin pathology was assessed by hematoxylin and eosin and toluidine blue staining and JAK2/STAT3 expression was detected by immunohistochemistry to determine the activation status of the related signaling pathway. The optimized formulation contained 4.45 g octadecanol, 4 g Vaseline, 2.2 g liquid paraffin, 0.81 g isopropyl myristate Estergel®, 1.6 g *Cnidium monnieri* volatile oil, 0.39 g sodium dodecyl sulfate, 1.16 g glycerol, 0.04 g nibergin ethyl ester and 25.35 g Distilled Water. *In vivo*, CMVOC markedly improved skin lesions in DNCB-induced mice, reduced serum IL-6 and IL-17 levels and alleviated epidermal thickening, edema and inflammatory infiltration. Immunohistochemistry further demonstrated suppressed activation of the JAK2-STAT3 signaling pathway. CMVOC effectively mitigated eczema-related inflammation by reducing pro-inflammatory cytokines and inhibiting JAK2-STAT3 pathway activation, providing experimental support for its potential as a topical therapy for eczema.

Correspondence to: Dr Ying Wang, College of Pharmacy, Shaanxi University of Chinese Medicine, 1, Middle Section of Century Avenue, Fengxi New Town, Xianyang, Shaanxi 712046, P.R. China
E-mail: wangying011@sntcm.edu.cn

Abbreviations: CMVO, *Cnidium monnieri* volatile oil; CMVOC, *Cnidium monnieri* volatile oil cream; DNCB, 2,4-dinitrochlorobenzene; ELISA, enzyme-linked immunosorbent assay; O/W, oil-in-water; W/O, water-in-oil; H&E, hematoxylin and eosin; GC-MS, gas chromatography-mass spectrometry

Key words: eczema, *Cnidium monnieri* volatile oil, cream formulation, anti-inflammation cytokine, JAK2-STAT3 signaling pathway

Introduction

Eczema is a prevalent chronic inflammatory skin condition characterized by recurrent episodes of erythema, papules and exudation, often accompanied by intense itching (1,2). Its etiology is multifactorial, involving complex interactions between neuro-immune-endocrine regulatory mechanisms in the skin and external triggers such as air pollution, house dust mites, water hardness and psychological stressors such as anxiety and depression (3-6). These factors collectively modulate local and systemic immune responses, with cytokines produced by the skin further influencing endocrine regulation. Epidemiological data indicate a prevalence of 10-25% in children and 5-10% in adults, with rates steadily increasing worldwide (7,8). Furthermore, most patients with eczema also have comorbid respiratory allergic conditions, such as asthma and hay fever (9). Genetic susceptibility is another significant factor, with heritability estimates reaching up to 80% in predisposed populations (10).

Current clinical management of eczema relies heavily on antibiotics, antihistamines and glucocorticoids, such as compound dexamethasone acetate cream (11). However, corticosteroid-based therapies are associated with multiple adverse effects, including local irritation, secondary infections and rebound symptoms upon abrupt discontinuation. Prolonged use may also lead to hyperpigmentation, skin atrophy and systemic reactions such as hypertension and hyperglycemia (12,13). Other drug classes, such as cyclosporine, are frequently linked to renal dysfunction, further limiting treatment options.

Given these limitations, *Cnidium monnieri* (Shechuangzi) has attracted increasing attention. Historically documented in the Divine Farmer's Classic of Materia Medica, this herb has been traditionally used to dispel wind and dampness (Zao Shi Qu Feng; anti-inflammatory and antipruritic, it

regulates the immune system and is mainly used for skin-related disorders and arthritis, etc.), relieve itching and treat parasitic skin conditions (14). Modern pharmacological studies have expanded its therapeutic profile, revealing antitumor, anti-inflammatory and anti-osteoporotic effects (15). The essential oil of *C. monnieri* is of particular interest due to its rich composition of bioactive sesquiterpenes and monoterpenes (16-20). Key components, including β-pinene and cnidicin, have been shown to antagonize histamine-induced responses, stabilize mast cells and inhibit mast cell degranulation, contributing to their anti-inflammatory and antibacterial effects (21-23). Moreover, *C. monnieri* volatile oil (CMVO) exhibits strong transdermal penetration, enhancing its suitability for topical treatment for eczema (24,25).

Despite its therapeutic potential, direct application of CMVO faces challenges due to its high volatility, susceptibility to light-induced degradation and potential for irritation from concentrated extracts (26,27). A review of topical delivery systems, including creams, patches and gels, suggests that cream formulations offer distinct advantages for essential oils (28,29). Creams can effectively improve stability, address the high lipophilicity of essential oils, enhance skin penetration and are simpler to prepare compared with other formulations. Based on these considerations, the present study incorporated CMVO into a cream formulation, optimized it using single-factor analysis and response surface methodology and evaluated its efficacy in a DNCB-induced mouse eczema model. The present study used ELISA, hematoxylin and eosin (H&E) staining, toluidine blue staining and immunohistochemistry to assess the anti-inflammatory effects of the optimized CMVOC. The present study aimed to develop a stable, safe, effective and quality-controlled topical preparation capable of alleviating eczema-associated inflammation and improving patient comfort.

Materials and methods

Reagents. The reagents used in this research included: octadecanol, sodium lauryl sulfate and ethyl nicotinate (Tianjin Kemiou Chemical Reagent Co., Ltd.); petrolatum (Shandong Dexinkang Medical Technology Co., Ltd.); liquid paraffin, isopropyl myristate (IPM), glycerol and acetone (Tianjin Tianli Chemical Reagent Co., Ltd.); compound dexamethasone acetate cream (China Resources Sanjiu Medical & Pharmaceutical Co., Ltd.); olive oil (Zhejiang Meizhiyuan Biotechnology Co., Ltd.); 2,4-dinitrochlorobenzene (DNCB; Chengdu Kelong Chemical Co., Ltd.); *Cnidium monnieri* (Shaanxi Xingshengde Pharmaceutical Co., Ltd.); ELISA Kit IL-6 (cat. no. MM-0163M1; Jiangsu Meimian Industrial Co., Ltd.); and ELISA Kit IL-17 (cat. no. MM-0170M1; Jiangsu Meimian Industrial Co., Ltd.); goat serum (cat. no. SL038; Beijing Solarbio Science & Technology Co., Ltd.); anti JAK2/STAT3 (cat.no. ab195055/ab31370; Abcam; HRP-labeled secondary antibody for goat anti-rabbit (cat. no. ab205718; Abcam); DAB staining (cat. no. DA1010; Beijing Solarbio Science & Technology Co., Ltd.). Additionally, the equipment used includes a GC-MS System (Agilent Technologies, Inc.), a PHS-3C pH meter (Shanghai INESA Scientific Instrument Co., Ltd.) and a rotational viscometer (cat. no. LC-NDJ-55; Shanghai Li-Chen Bang Xi Instrument Technology Co., Ltd.).

Laboratory animals. Male Kunming KM mice weighing 20-22 g were supplied by Chengdu Dasuo Laboratory Animal Co., Ltd. and the license number was SCXK (Chuan) 2025-0030. A total of 80 were purchased, among which 60 were used for pharmacodynamic tests (25 days) and 20 for safety tests (21 days). For the pharmacodynamic study, mice were allocated as described below. For serum-based analyses, six animals per group (n=6) were included based on sample availability following blood collection and the corresponding data are presented accordingly. Animal experiments were approved by the Shaanxi University of Chinese Medicine Laboratory Animal Ethics Committee (approval no. SUCMDL20250512001). Mice were housed in a laboratory with standard temperature (22±2˚C) and humidity (55±10%) under a 12-h light/dark cycle and underwent a 7-day acclimatization period. During the experiment, fresh drinking water was added and replaced daily. Animals were monitored daily for general health, behavior and signs of distress. Humane endpoints included severe weight loss (>20%), persistent ulceration, or inability to access food and water, upon which animals would be sacrificed immediately. After the experiment, 20 mice used for safety tests were sacrificed by cervical dislocation and 60 mice used for pharmacodynamics tests were intraperitoneally injected with 1% pentobarbital sodium (100 mg/kg). After the successful induction of anesthesia was confirmed by the righting reflex, ~1 ml of blood was collected from the eyeball and then sacrifice was performed by cervical dislocation. After the cervical dislocation sacrifice of the 80 mice, the breathing and pupil dilation conditions were observed to determine if the mice were dead.

Cream preparation. To minimize irritation and volatility, CMVO was incorporated into an ointment base. Oil-in-water (O/W) and water-in-oil (W/O) emulsion types were both screened to identify formulations with high gloss, fine smooth particles, light texture and excellent stability.

Formulations (Table I) were prepared by weighing the oil and aqueous phases separately. Each phase was heated separately in an 80˚C water bath until dissolved. The two phases were continuously stirred to achieve uniform mixing. Once they reached the same temperature, the aqueous phase was slowly poured into the oil phase while stirring continuously in the same direction until emulsification was complete. The emulsion was then cooled with continued stirring to room temperature until the cream formed.

A single-factor experiment was designed to investigate the optimal quantities of the aqueous and oil phases, as well as the base components with significant influence. Subsequently, a response surface experiment was conducted to derive the optimal formulation.

Composition of the prescription. Based on a literature review, four ointment formulations were selected for comparison (30-33). Formulation 1 and Formulation 2 were O/W types, while Formulation 3 and Formulation 4 were W/O types. Specific ingredients are shown in Table I.

Prescription optimization. Preliminary quality assessment of the four selected prescriptions indicated that Prescription 2 demonstrated the most effective results.

Table I. Prescription screening.

Ingredients	Prescription 1/g	Prescription 2/g	Prescription 3/g	Prescription 4/g
Stearic acid	6.00	/	6.00	15.10
Paraffinum molle	2.00	4.00	10.00	10.20
Octadecyl	/	3.60	/	/
Tween 80	3.00	/	/	5.00
Liquid paraffin	/	2.20	/	/
Glyceryl monostearate	/	/	2.00	10.00
Pan 80	/	/	/	2.00
IPM	/	1.00	/	/
Triethanolamine	3.00	/	0.40	/
PEG-400	3.00	/	/	/
Glycerinum	/	1.16	5.00	20.00
Lauryl sodium sulfate	/	0.30	/	/
Sorbic acid	/	/	/	0.20
Nibkin ethyl ester	/	0.04	0.10	/
Distilled water	/	27.40	45.00	37.50

IPM, isopropyl myristate.

Table II. Single-factor design (n=3).

Level	A/g	B/g	C/g	D/g	E/g	F/g
1	3.20	3.20	1.40	0.60	0.20	0.36
2	3.60	3.60	1.80	0.80	0.30	0.76
3	4.00	4.00	2.20	1.00	0.40	1.16
4	4.40	4.40	2.60	1.20	0.50	1.56
5	4.80	4.80	3.00	1.40	0.60	1.96

Table III. Response surface design (n=3).

Level	A/g	B/g	C/g
1	4.00	0.60	0.30
2	4.40	0.80	0.40
3	4.80	1.00	0.50

Single-factor analysis. To further refine the formulation ratio, a five-level single-factor experiment (n=3) was conducted to evaluate six components in the ointment formulation. Factors were labeled as follows: (A) octadecanol, (B) petrolatum, (C) liquid paraffin, (D) IPM, (E) sodium lauryl sulfate and (F) glycerin. The specific experimental design is shown in Table II.

Response surface design. Components markedly influencing cream stability were selected for re-evaluation. Three levels were chosen for each factor: (A) petrolatum, (B) IPM and (C) sodium lauryl sulfate. The Box-Behnken response surface method was employed using Design-Expert 13 software (Stat-Ease, Inc.) to arrange the experimental design (n=3). The design results are shown in Table III.

Quality evaluation. The cream was evaluated based on four major criteria, including the cream's appearance, droplet size, physical stability and moisturizing properties (34-36) and scored according to established standards with a maximum composite score of 100 points. The breakdown was as follows: Appearance and texture: 30% (each sub-criterion accounts for 5%); physical stability: 30% (each sub-criterion accounts for 10%); emulsion droplet size: 20% (each sub-criterion accounts for 10%); and moisturizing properties: 20%.

Appearance characteristics. The cream was expected to have a uniform texture and color, with appropriate viscosity for smooth application and absorption, free from noticeable particles or separation. Appearance characteristics were subdivided into five indicators: Sensory evaluation, gloss, particle size, skin feel and spreadability, each scored according to established standards. Specific criteria are detailed in Table IV.

Physical stability. The physical stability of the cream was evaluated through three indicators: Centrifugal stability, heat resistance and cold resistance. Scoring criteria are shown in Table V.

Centrifugal stability. For this test, 1 ml of the cream sample was placed into a 1.5 ml centrifuge tube and centrifuged at 735 x g for 30 min (25±2˚C). Oil-water separation was observed and scores were determined accordingly.

Heat stability. For this test, 7.5 g of the cream sample was placed in a 25 ml beaker, sealed with plastic wrap and placed in a 60˚C constant-temperature oven for 6 h. After cooling to room temperature, signs of oil-water separation, demulsification, or flocculation were observed.

Table IV. Evaluation criteria for appearance characteristics.

Standard	Score
Highly glossy, smooth and non-grainy, refreshing and easy to apply	5-6 points
Moderate gloss, with a slight grainy texture and a medium level of difficulty in application.	3-4 points
Dull, rough with a noticeable grainy texture, greasy and difficult to spread	<3 points

Table V. Physical stability evaluation criteria.

Standard	Score
No significant change	8-10 points
No separation, no oil or water separation, cream texture slightly soft or slightly firm	5-8 points
No separation, slight oil or water separation, cream texture too soft or too hard	3-6 points
Demulsification and separation	<3 points

Table VI. Evaluation criteria for droplet diameter.

Standard	Score
Small particle size with uniform distribution	7-10 points
Particle size is moderately sized with a relatively uniform distribution (with minor variations in localized areas).	4-7 points
Particle size is relatively large, with uneven distribution (dispersed or locally concentrated).	<4 points

Cold stability. For this test,7.5 g of the cream sample was placed in a sealed bag, refrigerated at 4˚C for 2 h, then frozen at -20˚C for 24 h. After returning to room temperature, oil-water separation, demulsification, or flocculation was observed.

Droplet diameter. Smaller particle size and more uniformly distributed droplets indicated higher cream quality. First, a temporary mount was prepared by taking a small amount of the cream sample, spreading it evenly onto the center of a microscope slide and then covering it with a coverslip. Next, a drop of glycerol was placed at the center of the coverslip. Finally, the prepared samples were observed using a bright-field light microscope at a magnification of x400. Five non-overlapping fields per sample were selected for particle size measurement by scanning the slide in a systematic manner (from left to right and top to bottom) to minimize selection bias. Droplet size and distribution were evaluated according to the criteria shown in Table VI.

Moisturizing properties. A cream sample (1 g) was weighed onto a microscope slide. After reweighing, the slide was placed in a 37˚C constant-temperature oven for 8 h. After removal and reweighing, the moisture loss rate and final score were calculated.

Determination of pH. At room temperature, 1 g of the cream was weighed, 10 g of purified water was added and the mixture was stirred evenly to form a white emulsion. The pH value was then measured using a pH meter. Three parallel determinations were conducted.

Determination of viscosity. Using a rotational viscometer, the 4th rotor was selected and the rotational speed was adjusted to 6 rpm. The instrument was started and the data were read once stabilized.

Extraction of CMVO. Volatile oil from *C. monnieri* was extracted using steam distillation. The raw material was ground into powder and 300 g of *C. monnieri* powder, which was identified by Professor Yonggang Yan from the College of Pharmacy, Shaanxi University of Chinese Medicine as the dried ripe fruit of *C. monnieri* (L.) Cuss. of the Apiaceae family, was placed into a 2,000 ml round-bottom flask with 1,300 ml of distilled water. After thorough mixing, the essential oil collection apparatus was assembled. Extraction was conducted via steam distillation for 6 h, ceasing when the product yield no longer increased. After cooling, the essential oil was collected, with an average yield of 1.06% (v/w). Three independent batches were extracted and GC-MS analysis demonstrated consistent chemical profiles among batches. The instrument used in Gas Chromatography-Mass Spectrometry (GC-MS) was a 7890GC/5977MS, (Agilent Technologies, Inc.). The EI ion source had an ionization energy of 70 eV and an initial temperature of 40˚C. It then gradually rose to 90˚C, followed by an increase at a rate of 5˚C per minute to 260˚C, which was maintained for 1 min. Subsequently, it was raised at a rate of 10˚C per minute to 260˚C; this process lasted for 6 min. The carrier gas used was high-purity helium with a flow rate of 1 ml/min.

DNCB-induced mouse eczema model. A total of 60 male specific pathogen-free (SPF)-grade mice were randomly divided into six groups of 10 mice each: Control, model, positive and low-, medium- and high-dose groups of *Cnidium monnieri* essential oil ointment. All animals were subjected to the same experimental procedures for model establishment and treatment. However, for serum-based analyses, a subset of animals (n=6 per group) was used and the corresponding data are presented accordingly. One day prior to modeling, depilation was performed on the dorsal region of mice in all groups except the normal group, covering an area of ~2 cm x 2 cm. On Day 1, all mice except the normal group were sensitized with 100 μl of a 7% DNCB solution in acetone:olive oil (4:1). A booster dose was administered on Day 2 and the challenge was repeated on Day 3. Starting on Day 4, except for the control group, mice were challenged with 30 μl of a 0.5% DNCB acetone-olive oil solution on the back every other day for a total of four challenges. After successful establishment of the eczema model, the normal group received daily application of 100 μl acetone-olive oil solution on the back. The model group received 100 μl of an unloaded cream formulation (100 mg/kg/d), the positive control group received 100 μl of compound dexamethasone acetate ointment (100 mg/kg/d) and the three groups treated with CMVOC received 100 μl of the corresponding dose of cream formulation (the dosage of CMVO in the cream): Low dose (100 mg/kg/d), medium dose (200 mg/kg/d) and high dose (400 mg/kg/d). Each group received twice-daily applications for 15 consecutive days. The precise dosage of the drug was derived by integrating multiple previous studies on local essential oil formulations, preliminary experiments and clinical dose conversions using the fingertip unit method (37-40). On the final day of the experiment, mice were fasted and deprived of water for 12 h. Blood samples were then collected from the eyeballs, skin samples were obtained from the dorsal region and changes in skin condition were observed. The severity of skin lesions was recorded on days 4, 7, 10, 13 and 16. Following the scoring principles of the EASI clinical scoring system (41), erythema, edema/thickening, scratches/erosions and crusting were selected as evaluation criteria. Scores were assigned on a scale of 0-3, where 0 indicated none (not present even upon close inspection), 1 indicated mild (related lesions visible upon close inspection), 2 indicated moderate (lesions directly visible) and 3 indicated severe (symptoms very pronounced). Based on the score, if the average score reaches 2 points and the model group remains above 2 points, it can be determined that the modeling is successful.

Safety inspection. A total of 20 male SFP-grade KM mice were randomly divided into four groups of five mice each: Control group, experimental group 1 (low-dose group), experimental group 2 (medium-dose group) and experimental group 3 (high-dose group) (all consisting of the CMVOC). After random grouping, all mice had their backs and the sides of their spines shaved (~2 cm x 2 cm). At 24 h later, skin scratches were made on the left side of the skin, while the right side was scratched in an equal shape to cause slight bleeding on the skin surface. The medication was applied immediately after the scratches. The normal group was applied with pure water and the experimental groups were applied with low-, medium- and high-dose groups of CMVOC. After administration, the mice were covered with gauze and fixed with adhesive tape. The medication was applied once a day. At 24 h later, the skin was washed with distilled water. After 1 h of cleaning, the mice were observed for 7 consecutive days for redness, swelling, or other phenomena. After stopping the medication, the mice were observed for another 7 days (42).

According to the scoring criteria in Table VII, the condition of the mouse's back skin was scored. The intensity of irritation was determined using the average scoring formula for the animals, according to Table VIII.

Determination of IL-6 and IL-17 by ELISA. Mouse serum samples were tested using ELISA kits from Jiangsu Enzyme Immunoassay Industrial Co., Ltd. IL-6 and IL-17 levels were determined according to the instruction manual. Intra-assay and Inter-assay coefficient of variation (CV) <15%. Standard curves were established and the concentration of each sample group was calculated. The standard curves for i) IL-17 and ii) IL-6 were as follows: i) $y=0.0047x + 0.0659$ $R^2=0.9957$; ii) $y=0.0039x + 0.1644$ $R^2=0.991$. Blood samples were collected from mice for serum preparation. During sample processing, four serum samples in the control group (K2, K3, K5 and K6) were affected by hemolysis due to technical issues during orbital blood collection and were therefore excluded from ELISA analysis.

As a result, six valid serum samples remained in the control group. Accordingly, ELISA analyses were conducted using six samples per group. For each treatment group, six serum samples were included in the analysis.

Serum levels of IL-6 and IL-17 were measured using commercial ELISA kits according to the manufacturers' instructions. All assays were performed following standard protocols and no samples were excluded based on experimental outcomes.

H&E staining. Fresh skin tissue was fixed in 4% paraformaldehyde solution for 24 h (25±2˚C), routinely embedded in paraffin (25±2˚C) and sectioned into 4 μm-thick slices (-20˚C). The sections underwent dewaxing (65˚C) and hydration with a gradient of ethanol (100, 95, 80 and 75%), followed by rinsing with distilled water. Sections were immediately immersed in hematoxylin stain for 5 min, rinsed with tap water for 1 min, deparaffinized with hydrochloric acid ethanol for 30 sec, soaked in tap water for 15 min and then placed in eosin solution for 2 min. After staining, sections were re-washed with graded ethanol and clarified with xylene. Finally, neutral resin was applied to mount the sections (25±2˚C). Once dried, the sections were ready for bright-field light microscopic examination (43). The tissue morphology was observed under a bright-field light microscope at a magnification of x200 and images were captured. A total of three non-overlapping fields per sample were selected for cell counting by scanning the slide in a systematic manner (from left to right and top to bottom) to minimize selection bias.

Toluidine blue staining. The pretreatment procedure was identical to that for H&E staining: Tissue fixation, dehydration, clearing, paraffin embedding, sectioning and dewaxing. The prepared sections were placed in a 0.5% toluidine blue solution

Table VII. Skin safety rating criteria.

Skin reaction	Score
Degree of erythema	
No erythema	0
Mild erythema	1
Marked erythema	2
Moderate erythema	3
Severe erythema with slight eschar formation	4
Degree of edema	No edema
No edema	0
Mild edema	1
Marked edema, i.e., clearly visible skin swelling	2
Moderate edema, i.e., elevation of ~1 mm	3
Severe edema, with elevation exceeding 1 mm	4
Highest score	8

Table VIII. Skin irritation severity classification criteria.

Average score	Strength
0-0.5	Non-irritating
0.5-2	Mildly irritating
2-6	Moderately irritating
6-8	Strongly irritating

and incubated at 55˚C for 20 min. After 2-3 rinses with water, the sections were placed in hydrochloric acid alcohol for 2-3 sec for decolorization, followed by rinsing with water. Dehydration was performed using alcohol and the sections were then stained with 0.25% eosin for 8 sec (25±2˚C). Finally, routine procedures of decolorization, dehydration, clearing and mounting were carried out sequentially. After air-drying, the sections were observed under a microscope (44).

Immunohistochemistry. Mouse skin tissue sections of 2-5 μm were processed dewaxing, rehydration, xylene and graded ethanol treatments. Next, antigen retrieval was performed using the citric acid antigen retrieval buffer (pH 6.0) and then using an electric pressure cooker. Following three washes with TBS, the sections were incubated with 0.1% Triton X-100 for 10 min, reacted with 0.3% H_2O_2 in methanol at room temperature (25±2˚C) for 30 min then blocked with 10% goat serum (cat. no. SL038; Beijing Solarbio Science & Technology Co., Ltd.) in PBS for 10 min at room temperature. When adding the primary antibody, gently shake off the blocking solution. Sections were incubated with primary antibody of JAK2/STAT3 (cat. no. ab195055/ab31370; Abcam) diluted 1:200 in PBS onto the slide at 4˚C for 24 h. The slide was placed in PBS (pH 7.4) and shaken three times, each time for 5 min. After slightly drying the slide, the secondary antibody of HRP-labeled goat anti-rabbit (cat. no. ab205718; Abcam) corresponding to the species of the secondary antibody was added to the slide at a ratio of 1:500 to cover the tissue and incubated at room temperature for 50 min. The slide was placed in PBS (pH 7.4) and shaken three times, each time for 5 min. Following DAB staining at room temperature (25±2˚C; cat. no. DA1010; Beijing Solarbio Science & Technology Co., Ltd.), under microscopic observation until brownish-yellow staining appeared, the sections were rinsed with tap water to terminate the color development reaction. Sections were counterstained with hematoxylin (25±2˚C, 3 min), dehydrated, cleared and mounted. Processed sections were examined under a bright-field light microscope (45,46).

Statistical analysis. Experimental data in the present study were processed using GraphPad Prism 10.4.2 software (Dotmatics). Results from single-factor experiments and response surface experiments in the cream base screening were expressed as means, with n=3. For mouse data in the eczema model experiments, serum-based analyses were performed using six animals per group (n=6).

Quantitative data from animal studies were expressed as mean ± standard deviation. Prior to statistical analysis, data were assessed for normality using the Shapiro-Wilk test and for homogeneity of variances using Levene's test.

For datasets meeting the assumptions of normality and homogeneity of variance, statistical comparisons among multiple groups were performed using one-way analysis of variance followed by Tukey's post hoc test. For datasets with unequal variances or unequal sample sizes, Welch's ANOVA followed by Games-Howell multiple comparisons test was applied. This approach ensures that statistical analyses accurately reflect the experimental design, regardless of unequal variances or deviations from normality.

Histological and immunohistochemical data, including epidermal thickness, mast cell counts, H&E staining, toluidine blue staining and immunohistochemistry, were quantified using ImageJ-win64 software (National Institutes of Health). By including all pre-defined animals and using appropriate statistical methods, the analyses were both transparent and unbiased. $P<0.05$ was considered to indicate a statistically significant difference.

Results

GC-MS analysis. The active components of *Cnidium monnieri* essential oil were analyzed using GC-MS. The total ion chromatogram is presented in Fig. 1. By comparing with the NIST database and retention indices, 21 active compounds were identified as listed in Table IX, with their chemical structures depicted in Fig. 2.

Preparation of cream

Single-factor analysis experiment. Fig. 3 illustrates the effect of varying base component levels on the final evaluation scores. Octyldodecanol, IPM and sodium lauryl sulfate markedly influenced the scores. Among these, octyldodecanol (4.40 g) provided optimal cream stability; lower levels led to oil-water separation, while higher levels resulted

Table IX. Active components of *Cnidium monnieri* volatile oil.

No.	Compound	CAS	Total, %
1	Butanoic acid, 2-methyl-, 1-methylethyl ester	066576-71-4	0.836
2	(1R)-2,6,6-Trimethylbicyclo[3.1.1]hept-2-ene	007785-70-8	25.585
3	Camphene	000079-92-5	9.976
4	Bicyclo[3.1.0]hexane, 4-methylene-1-(1-methylethyl)-	003387-41-5	1.363
5	Bicyclo[3.1.1]heptane, 6,6-dimethyl-2-methylene-, (1S)-	018172-67-3	3.01
6	D-Limonene	005989-27-5	22.22
7	Cyclohexene, 1-methyl-4-(1-methylethylidene)-	000586-62-9	0.766
8	endo-Borneol	000507-70-0	1.366
9	Estragole	000140-67-0	1.469
10	Bicyclo[2.2.1]heptan-2-ol, 1,7,7-trimethyl-, acetate, (1S-endo)-	005655-61-8	14.792
11	Caryophyllene	000087-44-5	1.387
12	(1R,2S,6S,7S,8S)-8-Isopropyl-1-methyl-3-methylenetricyclo [4.4.0.02,7]decane-rel-	018252-44-3	0.6
13	trans-α-bergamotene	013474-59-4	0.885
14	Perillyl isobutyrate	1000429-32-1	3.265
15	Hexadecane	000544-76-3	0.525
16	(6E)-8-Methyl-6-nonenoic acid	059320-77-3	1.16
17	Bicyclopentyl-1,1'-diene	000934-02-1	4.222
18	Chrysantenyl 2-methuylbutanoate	053820-13-6	0.628
19	cis-Chrysanthenyl propionate	070470-69-8	0.832
20	2-Cyclohexen-1-ol, 2-methyl-5-(1-methylethenyl)-, propanoate	000097-45-0	2.185
21	Osthole	000484-12-8	2.929

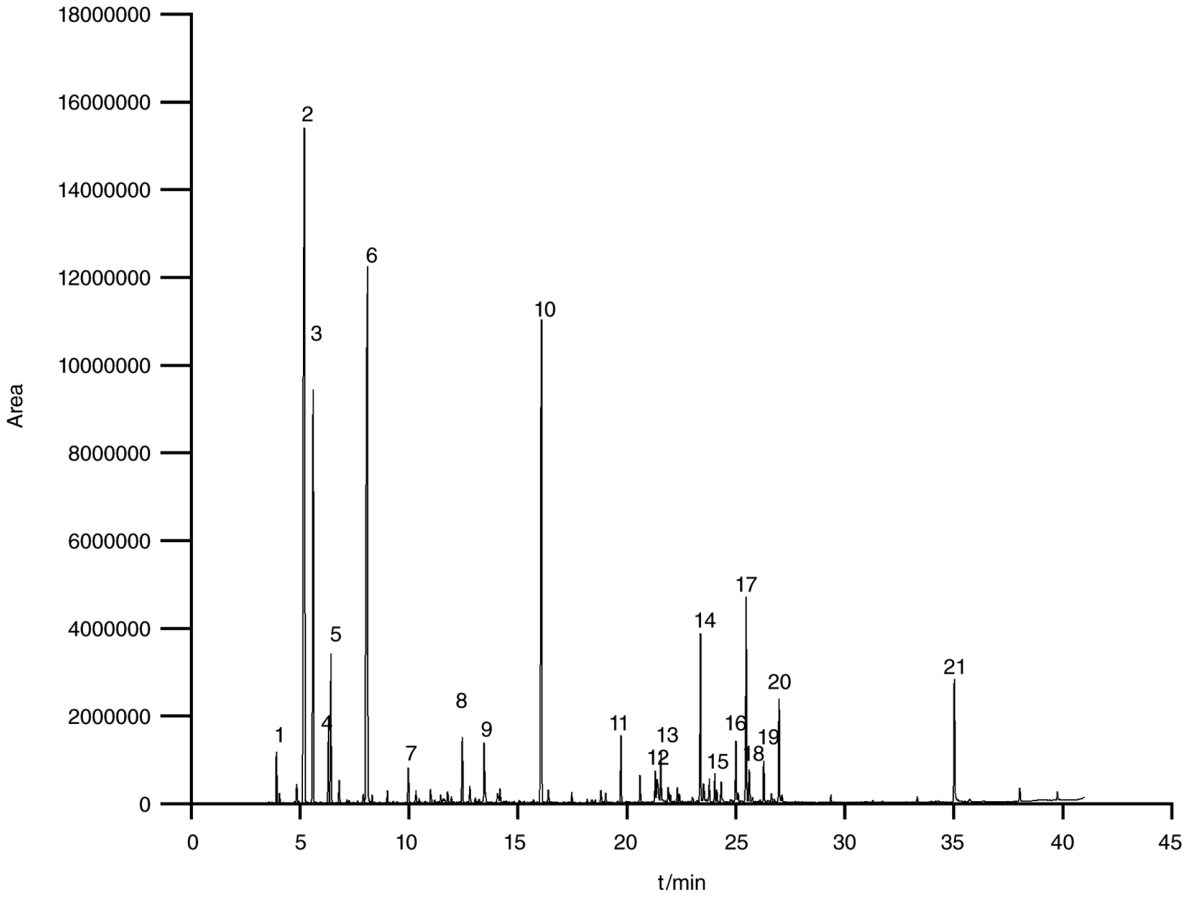

Figure 1. GC-MS Analysis of CMVO. GC-MS, gas chromatography-mass spectrometry; CMVO, *Cnidium monnieri* volatile oil.

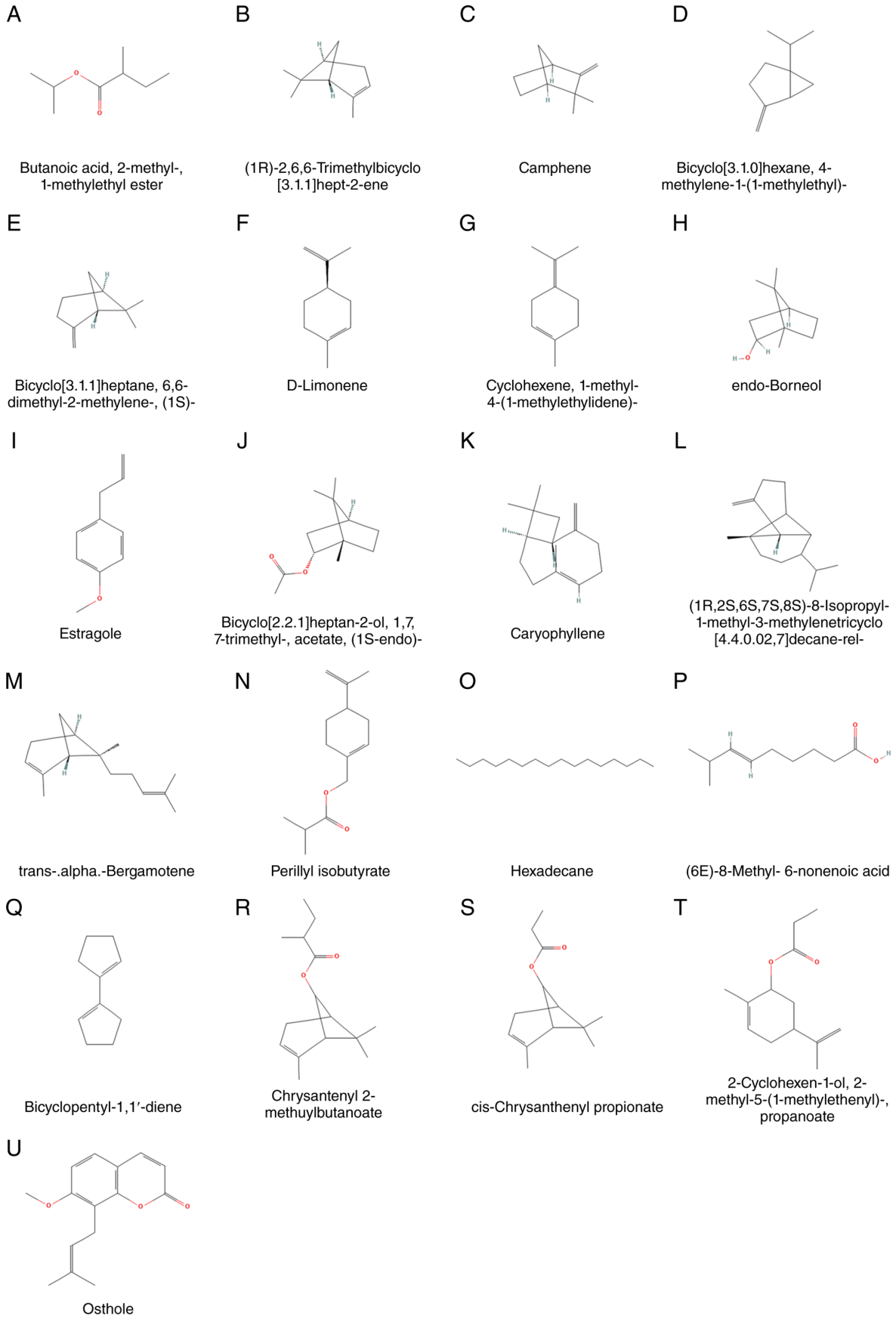

Figure 2. Compound structure. (A) Butanoic acid, 2-methyl-, 1-methylethyl ester; (B) (1R)-2,6,6-Trimethylbicyclo[3.1.1] hept-2-ene; (C) Camphene; (D) Bicyclo[3.1.0]hexane, 4-methylene-1-(1-methylethyl)-; (E) Bicyclo[3.1.1]heptane, 6,6-dimethyl-2-methylene-, (1S)-; (F) d-limonene; (G) Cyclohexene, 1-methyl-4-(1-methylethylidene)-; (H) endo-borneol; (I) Estragole; (J) Bicyclo[2.2.1] heptan-2-ol, 1,7,7-trimethyl-, acetate, (1S-endo)-; (K) Caryophyllene; (L) (1R,2S,6S,7S,8S)-8-Isopropyl-1-methyl-3-methylenetricyclo[4.4.0.02,7] decane-rel-; (M) trans-α-Bergamotene; (N) Perillyl isobutyrate; (O) Hexadecane; (P) (6E)-8-Methyl-6-nonenoic acid; (Q) Bicyclopentyl-1,1'-diene; (R) Chrysantenyl 2-methuylbutanoate; (S) cis-Chrysanthenyl propionate; (T) 2-Cyclohexen-1-ol, 2-methyl-5-(1-methylethenyl)-, propanoate; (U) Osthole)

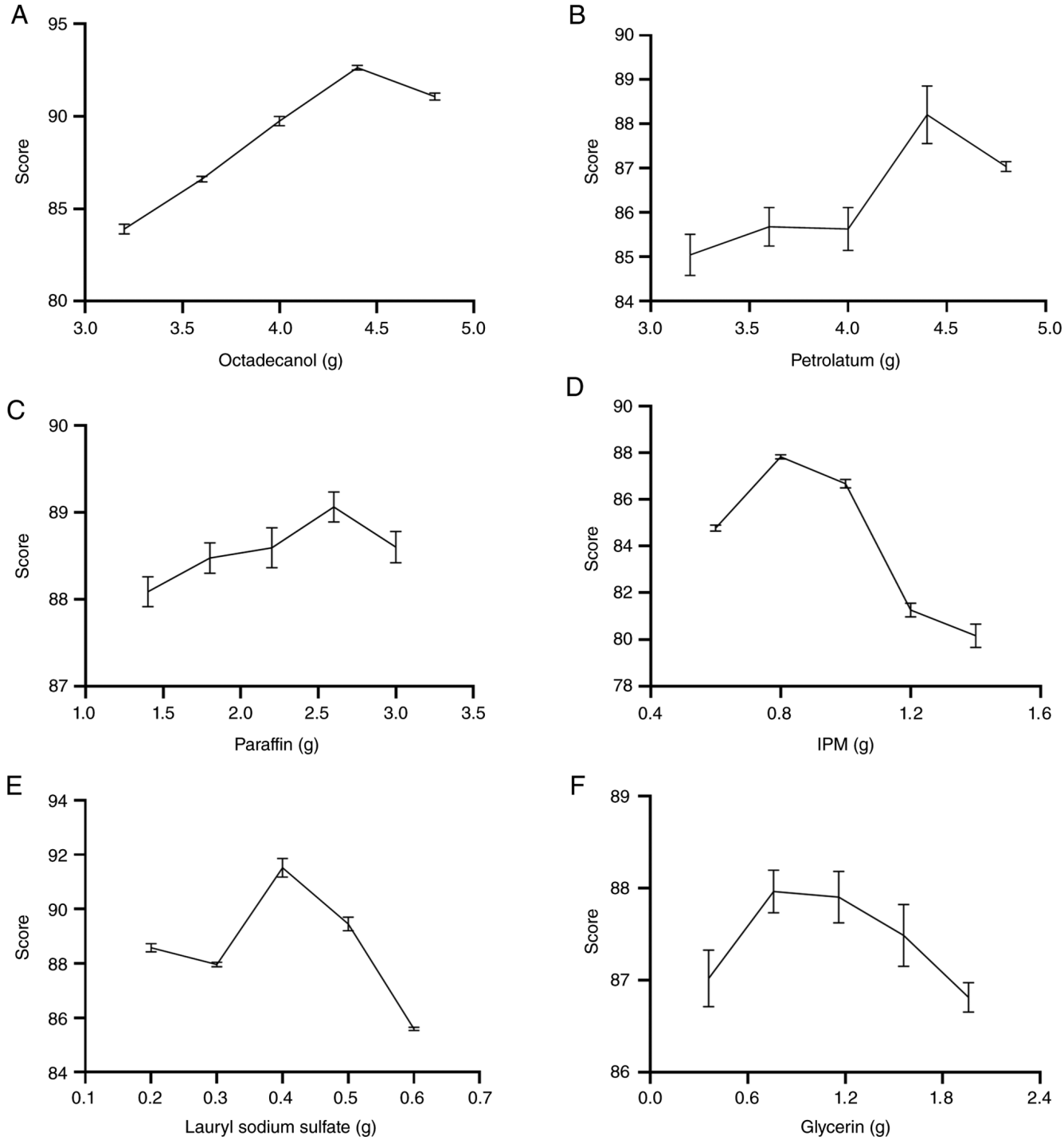

Figure 3. Single-factor trend analysis. (A) Octadecanol; (B) paraffinum molle; (C) liquid paraffin; (D) IPM; (E) lauryl sodium sulfate; (F) glycerin. IPM, isopropyl myristate.

in hard, difficult-to-spread creams. IPM (0.80 g) exhibited optimal skin affinity; lower concentrations caused excessive greasiness, while higher levels disrupted the cream structure, leading to a granular texture. Sodium lauryl sulfate (0.40 g) achieved maximum emulsifying efficacy; lower concentrations prevented cream formation, while higher levels increased viscosity. By contrast, petrolatum, liquid paraffin and glycerin exhibited markedly lower variability, with no significant changes observed across their five respective concentration levels. As lubricants and moisturizers, their moderate dosages exerted no discernible effect on the cream formulation. The experimental variables comprised (A) octadecanol, (B) petrolatum, (C) liquid paraffin, (D) IPM, (E) lauryl sodium sulfate and (F) glycerin, with detailed experimental procedures and results outlined in Tables X and XI.

Experimental results of response surface optimization

Response surface experiment results. A Box-Behnken response surface design was conducted using Design-Expert

Table X. Single-factor experiment score distribution (n=3).

Group	External properties					Stability			Particle size		Moisture retention	Score
	Sense	Glossiness	Granularity	Skin feeling	Coating property	Centrifugal stability	Heatproof level	Cold-resistance	Size	Distribution		
A1	5.82	5.90	5.77	5.83	5.78	9.80	7.47	4.13	8.30	7.60	17.51	83.91
A2	5.69	5.95	5.78	5.70	5.61	9.80	8.88	4.95	8.20	8.00	18.05	86.60
A3	5.91	5.93	5.83	5.86	5.82	9.80	8.43	7.55	8.65	8.51	17.44	89.74
A4	5.84	5.94	5.89	5.83	5.92	9.80	9.61	8.87	8.84	8.67	17.41	92.63
A5	5.69	5.83	5.85	5.70	5.63	9.80	9.59	8.42	8.41	8.30	17.86	91.07
B1	5.74	5.91	5.91	5.82	5.65	9.80	8.33	4.53	7.85	8.29	17.21	85.04
B2	5.85	5.95	5.92	5.91	5.89	9.80	8.50	4.50	8.30	7.56	17.49	85.68
B3	5.80	5.95	5.92	5.88	5.81	9.80	8.50	4.53	7.53	8.27	17.63	85.63
B4	5.83	5.95	5.93	5.88	5.87	9.80	8.98	6.07	8.00	7.93	17.97	88.21
B5	5.78	5.95	5.92	5.84	5.81	9.80	7.42	6.60	7.80	7.81	18.31	87.04
C1	5.83	5.95	5.93	5.79	5.82	9.80	8.76	5.52	8.01	7.96	18.72	88.09
C2	5.84	5.95	5.93	5.84	5.84	9.80	9.37	5.87	7.50	8.30	18.24	88.48
C3	5.85	5.95	5.94	5.82	5.73	9.80	8.73	5.47	8.00	8.41	18.89	88.59
C4	5.85	5.95	5.95	5.87	5.88	9.80	8.57	5.77	8.60	8.45	18.38	89.06
C5	5.76	5.94	5.95	5.70	5.80	9.80	7.38	6.89	8.30	8.20	18.89	88.60
D1	5.76	5.94	5.96	5.76	5.81	9.80	7.32	8.45	6.91	5.12	17.95	84.78
D2	5.78	5.93	5.82	5.95	5.83	9.80	9.11	7.39	7.50	6.81	17.91	87.82
D3	5.78	5.80	5.82	5.86	5.83	9.80	8.24	7.89	7.50	6.58	17.56	86.67
D4	5.76	5.93	5.78	5.85	5.85	9.80	8.99	9.22	3.00	3.00	18.09	81.27
D5	5.79	5.93	5.91	5.75	5.69	9.80	8.66	8.23	3.20	3.50	17.70	80.17
E1	5.77	5.80	5.81	5.91	5.84	9.80	9.21	9.35	6.89	6.67	17.53	88.58
E2	5.70	5.93	5.95	5.70	5.65	9.80	8.62	5.03	8.52	8.34	18.71	87.96
E3	5.90	5.86	5.88	5.75	5.79	9.80	9.30	8.10	8.12	8.30	18.72	91.52
E4	5.82	5.93	5.92	5.79	5.81	9.80	9.13	6.13	8.39	7.70	19.03	89.45
E5	5.78	5.80	5.82	5.84	5.86	9.80	8.12	7.35	7.01	6.57	17.66	85.60
F1	5.63	5.93	5.87	5.57	5.63	9.80	8.97	6.23	7.64	7.43	18.31	87.02
F2	5.69	5.93	5.90	5.62	5.64	9.80	9.13	6.59	7.82	7.43	18.40	87.96
F3	5.76	5.93	5.92	5.72	5.72	9.80	9.23	7.53	6.80	7.21	18.28	87.90
F4	5.72	5.93	5.86	5.68	5.68	9.80	9.45	6.28	7.56	7.10	18.44	87.49
F5	5.63	5.93	5.89	5.60	5.58	9.80	8.92	6.64	7.55	6.95	18.33	86.81

Table XI. Single-factor experiment results (n=3).

Level	A	B	C	D	E	F
1	83.91	85.04	88.09	84.78	88.58	87.02
2	86.60	85.68	88.48	87.82	87.96	87.96
3	89.74	85.63	88.59	86.67	91.52	87.90
4	92.63	88.21	89.06	81.27	89.45	87.49
5	91.07	87.04	88.60	80.17	85.60	86.81

Table XII. Response surface experiment results.

Standard	Run	A	B	C	Score
7	1	4.00	0.80	0.50	85.55
14	2	4.40	0.80	0.40	91.63
9	3	4.40	0.60	0.30	86.59
15	4	4.80	0.80	0.30	91.58
3	5	4.00	1.00	0.40	85.72
17	6	4.80	0.80	0.50	92.15
11	7	4.40	0.60	0.50	86.18
4	8	4.80	1.00	0.40	87.07
12	9	4.40	1.00	0.50	86.42
13	10	4.40	0.80	0.40	92.48
16	11	4.40	0.80	0.40	92.26
6	12	4.80	0.80	0.30	87.61
5	13	4.00	0.80	0.30	85.98
10	14	4.40	1.00	0.30	87.52
8	15	4.80	0.80	0.50	86.95
1	16	4.00	0.60	0.40	84.14
2	17	4.80	0.60	0.40	86.35

13 software. The experimental details and results are shown in Table XII.

Model fitting and analysis of variance. Based on the experimental scores, regression analysis yielded the following multiple quadratic regression equation: $Y=92.02 + 0.8238^{*}A + 0.4338^{*}B-0.3250^{*}C-0.2150^{*}$ $AB-0.0575^{*}AC-0.1725^{*}BC-3.18^{*}A^{2}-3.02^{*}B^{2}-2.32^{*}C^{2}$.

The results of the analysis of variance are presented in Table XIII. The model was significant (P<0.0001), with a non-significant lack-of-fit term (P=0.7267>0.05), indicating that the model fitted well with minimal interference from other factors. Additionally, $R^{2}=0.9932$ and adjusted $R^{2}=0.9844$ further demonstrated the model's high accuracy. The F-value revealed the following influence order: octadecanol (A) > IPM (B) > sodium lauryl sulfate (C).

Model optimization and prediction. Based on the multiple quadratic regression equation, Design-Expert 13 was used to generate contour plots and response surfaces, which visually depicted the effect of factor interactions on cream scores, as illustrated in Fig. 4. These interactions further elucidated the intricate relationships within the formulation matrix. In the AB interaction, cream scores initially rose and then declined with increasing octadecyl alcohol content. Similarly, when IPM content rose, octadecanol scores followed an up-and-down pattern, suggesting a non-significant interaction between octadecyl alcohol and IPM. The highest score was attained at an octadecanol content of 4.00 g and an IPM content of 0.60 g. For the AC interaction, the score initially increased and subsequently decreased with rising sodium lauryl sulfate content. When sodium lauryl sulfate content increased, the trend of octadecyl alcohol scores remained unchanged, similarly indicating a non-significant interaction between the two. The highest score was recorded at an octadecanol content of 4.40 g and a sodium lauryl sulfate content of 0.40 g. In the BC interaction, both IPM and sodium lauryl sulfate content exhibited scores that initially increased and then decreased, pointing to a non-significant interaction between them. The highest score was achieved at an IPM content of 0.80 g and a sodium lauryl sulfate content of 0.40 g. Response surface prediction pinpointed the optimal formulation for preparing CMVO ointment: octadecanol at 4.45 g, IPM at 0.81 g and sodium lauryl sulfate at 0.39 g, yielding a comprehensive score of 92.10 points.

Verification of the optimal formulation. The total assessment scores are detailed in Table XIV. The average scores were 92.46±0.26, 92.48±0.2 and 91.48±0.27, closely aligning with the model-predicted value of 92.10. This demonstrated a strong concordance between the experimental results and the predicted values.

Quality evaluation

Appearance characteristics. As presented in Fig. 5, these are the appearances of four cream formulations. In the selection of a suitable cream, priority should be given to those with uniform texture, appropriate consistency and the absence of noticeable particles or separation.

Physical stability

Centrifugal stability. After centrifugation at 735 x g for 30 min (25±2˚C), none of the formulations exhibited oil-water separation, with no significant differences observed among groups. These findings demonstrate that the formulation exhibited good centrifugal stability.

Heat stability. Following storage at 60˚C for 6 h and subsequent cooling to room temperature, the cream maintained a uniform texture and color. It remained smooth, refreshing and easy to apply, without any signs of thinning, clumping, or oil-water separation, demonstrating the cream's good heat resistance.

Cold stability. After refrigeration at 4˚C for 2 h and freezing at -20˚C for 24 h, the cream exhibited no significant changes in color or texture upon returning to room temperature. It remained light, smooth and easy to apply, with no signs of thinning, clumping, or oil-water separation, confirming the cream's strong cold resistance.

Droplet diameter. Particle size measurements of the drug-loaded ointment revealed that 3 to 5 particle sizes

Table XIII. Response surface regression model analysis of variance.

Source	Sum of Squares	Degrees of freedom	Mean Square	F-value	P-value	
Model	123.63	9	13.74	113.32	<0.0001	Significant
A-octadecanol	5.43	1	5.43	44.78	0.0003	
B-IPM	1.51	1	1.51	12.42	0.0097	
C-lauryl sodium sulfate	0.8450	1	0.8450	6.97	0.0334	
AB	0.1849	1	0.1849	1.53	0.2567	
AC	0.0132	1	0.0132	0.1091	0.7508	
BC	0.1190	1	0.1190	0.9819	0.3547	
A^2	42.51	1	42.51	350.68	<0.0001	
B^2	38.47	1	38.47	317.30	<0.0001	
C^2	22.66	1	22.66	186.95	<0.0001	
Residual	0.8486	7	0.1212			
Lack of Fit	0.2168	3	0.0723	0.4575	0.7267	Not significant
Pure Errot	0.6318	4	0.1580			
Cor Total	124.48	16				

were marked in each group across low, medium and high dosage formulations (n=3). The average particle size was ~85.50±15.33 nm, meeting the preparation standard (ointment particle size <180 nm). The particle size distribution is detailed in Fig. 6 and Table XV.

pH. The pH of the cream was measured using a PHS-3C pH meter at different drug loading doses, with results shown in Table XV. After analysis, it can be seen that the average pH values for the low-, medium- and high-dose groups were 6.92±0.00, 6.91±0.02 and 6.91±0.01, respectively. Overall, the cream was weakly acidic, aligning with the pH range suitable for skin application.

Viscosity. Viscosity measurements conducted at room temperature, with results shown in Table XV, revealed similar viscosity values across different doses, with no significant difference observed. Moreover, this viscosity falls within the range suitable for external skin application, ensuring the cream's applicability and stability while preventing phenomena such as stratification.

Observation of mouse skin condition. A scoring system for assessing the severity of skin lesions in mice was established based on the EASI criteria, as detailed in Table XVI. On Day 4, mice exhibited mild eczema symptoms. From Days 7 to 10, symptoms intensified but remained below severe levels due to the administration of the medication. By Days 13 to 16, significant improvement was observed, indicating the medication's effectiveness in alleviating eczema symptoms. As illustrated in Fig. 7, following DNCB induction, mice displayed clear signs of eczema. However, treatment with CMVO ointment mitigated skin tissue damage. Visual inspection revealed that the control group's skin appeared pale pink without abnormalities, while the model group exhibited pronounced skin lesions and swelling, confirming successful DNCB-induced eczema modeling. All treatment groups showed marked improvements in skin condition. Although both the model and treated groups displayed skin lesions, redness, swelling and scabbing, the model group showed the most pronounced lesions and swelling. In the positive control group, scabs had completely fallen off, revealing pale pink skin without swelling or hyperemia. Mice in the low-dose cream group still exhibited slight redness and swelling, with limited desquamation of crusted areas. The medium-dose cream group exhibited partial crust desquamation, exposing pale pink skin, as did the high-dose cream group.

Analysis of security detection. As depicted in Fig. 8, mild erythema emerged in the high-dose group of the experimental group after seven days of use. Calculations revealed average scores per animal of 0.04 in the high-dose control group and 0.26 in the skin-lesion group, both below the 0.5 threshold. Based on these local irritation findings, the test was deemed non-irritating according to the scoring criteria. The specific scoring results are outlined in Table XVII.

Determination of IL-6 and IL-17 by ELISA. As shown in Fig. 9, the model group exhibited markedly elevated levels of the pro-inflammatory cytokines IL-6 and IL-17 compared with the normal group. By contrast, the positive control group and the medium- and high-dose groups of CMVO ointment showed marked reductions in these proinflammatory factors compared with the model group.

Skin dyeing. Figs. 10 and 11 depict the results of H&E staining and toluidine blue staining of mouse skin tissue, reflecting relevant pathological conditions. H&E staining results revealed that the skin structure in the normal group was intact, with no inflammatory cell infiltration in the dermis. By contrast, the model group showed thickening of the granular and spinous layers, intercellular edema and inflammatory cell infiltration in the dermis. Treatment with different drugs led to thinner

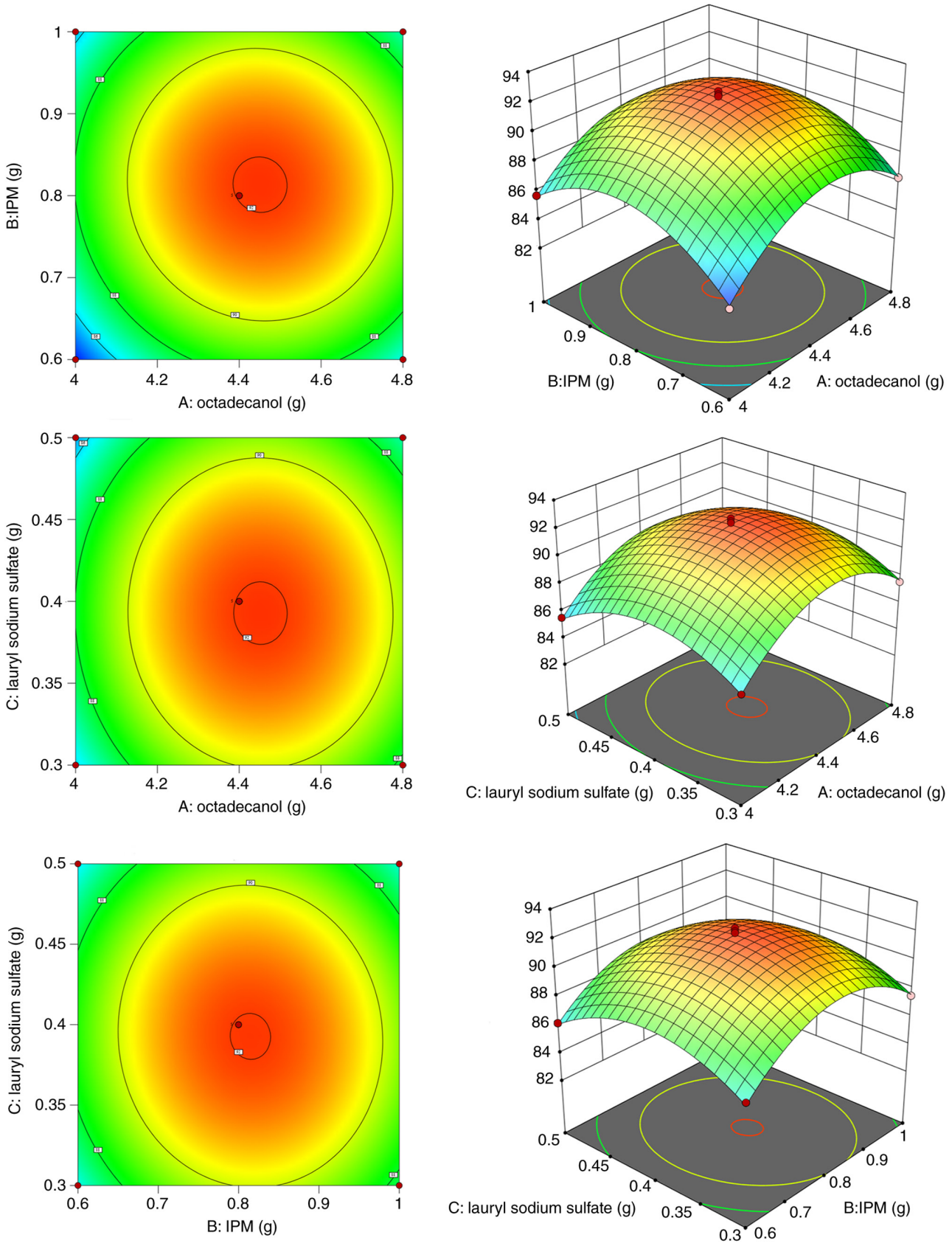

Figure 4. Contour plots of factor interactions and response surface plots. IPM, isopropyl myristate.

granular and spinous layers and a significant reduction in intercellular edema and inflammatory cell infiltration in the dermis.

Toluidine blue staining highlighted clear differences in mast cell distribution among the groups. The control group had very few, sparsely distributed mast cells, while the model

Table XIV. Results of validation experiments (n=3).

Group	External properties					Stability			Particle size		Moisture retention	Score
	Sense	Glossiness	Granularity	Skin feeling	Coating property	Centrifugal stability	Heatproof level	Cold-resistance	Size	Distribution		
1-1	5.58	5.91	5.52	5.63	5.74	9.80	8.91	9.54	8.92	8.53	18.13	92.21
1-2	5.51	5.91	5.43	5.65	5.78	9.80	8.79	9.51	8.99	8.79	18.27	92.43
1-3	5.59	5.91	5.61	5.69	5.75	9.80	8.95	9.46	9.01	8.85	18.11	92.73
2-1	5.65	5.91	5.47	5.51	5.67	9.80	8.71	9.15	9.35	8.58	18.48	92.28
2-2	5.72	5.91	5.51	5.69	5.83	9.80	8.96	9.07	9.21	8.63	18.34	92.67
2-3	5.64	5.91	5.36	5.67	5.82	9.80	8.85	9.22	9.27	8.69	18.26	92.49
3-1	5.21	5.91	5.52	5.50	5.69	9.80	9.59	9.36	8.47	8.26	18.42	91.73
3-2	5.51	5.91	5.17	5.49	5.64	9.80	9.29	9.18	8.53	8.31	18.37	91.20
3-3	5.41	5.91	5.23	5.47	5.68	9.80	9.34	9.27	8.91	8.25	18.25	91.52

group exhibited numerous densely clustered mast cells. After drug administration, the positive group demonstrated a significant reduction in mast cell numbers with a more scattered distribution. Among the different dosage groups, mast cell counts decreased progressively with increasing drug concentration.

Quantitative analysis of epidermal thickness and mast cell counts is presented in Fig. 12. Compared with the control group, the model group exhibited increased epidermal thickness ($P<0.0001$) and mast cell counts ($P<0.0001$). Compared with the model group, the treatment groups exhibited reduced epidermal thickness and mast cell counts ($P<0.0001$, $P<0.001$, $P<0.05$), reflecting the inflammatory status in each group.

Immunohistochemistry. Immunohistochemical staining revealed JAK2 expression as a brownish-yellow color in the cytoplasm, while STAT3 was detected in both the cytoplasm and nucleus, also displaying a brownish-yellow hue. In the normal group, JAK2 expression was weak, confined to the basal layer of the epidermis and hair follicles, while STAT3 remained inactive with minimal detectable staining. Compared with the normal group, the model group exhibited thickened stratum spinosum, with strong cytoplasmic JAK2 expression appearing as brownish-yellow. Infiltrating inflammatory cells in the superficial dermis exhibited brownish-gray staining. STAT3 showed both cytoplasmic brownish-yellow positivity and brownish-gray granular nuclear staining in inflammatory cells of the superficial dermis. Overall, JAK2 and STAT3 expression levels were markedly elevated in the model group. By contrast, all treatment groups demonstrated markedly reduced positive expression levels, narrower cytoplasmic distribution, lighter staining intensity and disappearance of STAT3 nuclear positive signals, indicating effective suppression of pathway activation following treatment.

Analysis of results is shown in Fig. 13. Compared with the normal control group, the model group exhibited markedly upregulated JAK2 and STAT3 signaling ($P<0.001$), indicating altered molecular expression of this pathway. Combined with H&E and toluidine blue staining results, these findings suggested that the eczema model successfully induced inflammation. Compared with the model group, the positive drug group and different doses of CMVOC administration groups showed significant differences in the molecular expression of JAK2 and STAT3 ($P<0.05$, $P<0.01$, $P<0.001$). These results suggested that the JAK2-STAT3 signaling pathway may be one of the mechanisms by which CMVOC alleviates eczema.

As illustrated in Fig. 14, JAK2 expression exhibited a brownish-yellow cytoplasmic staining pattern. In the normal group, JAK2 expression was minimal and distributed between the epidermis and dermis. Compared with the normal group, the model group showed such as upregulated JAK2-positive expression, with brownish-yellow cytoplasmic staining in epidermal spinous layer cells and abundant inflammatory cell infiltration in the dermis. Compared with the model group, the positive group exhibited downregulated JAK2 expression, with fewer brownish-yellow cytoplasmic cells and inflammatory cells in the dermis. Similarly, all low-, medium- and high-dose groups treated with CMVO ointment showed downregulated JAK2 signal expression, with significant differences compared with the model group, particularly in the medium- and high-dose groups.

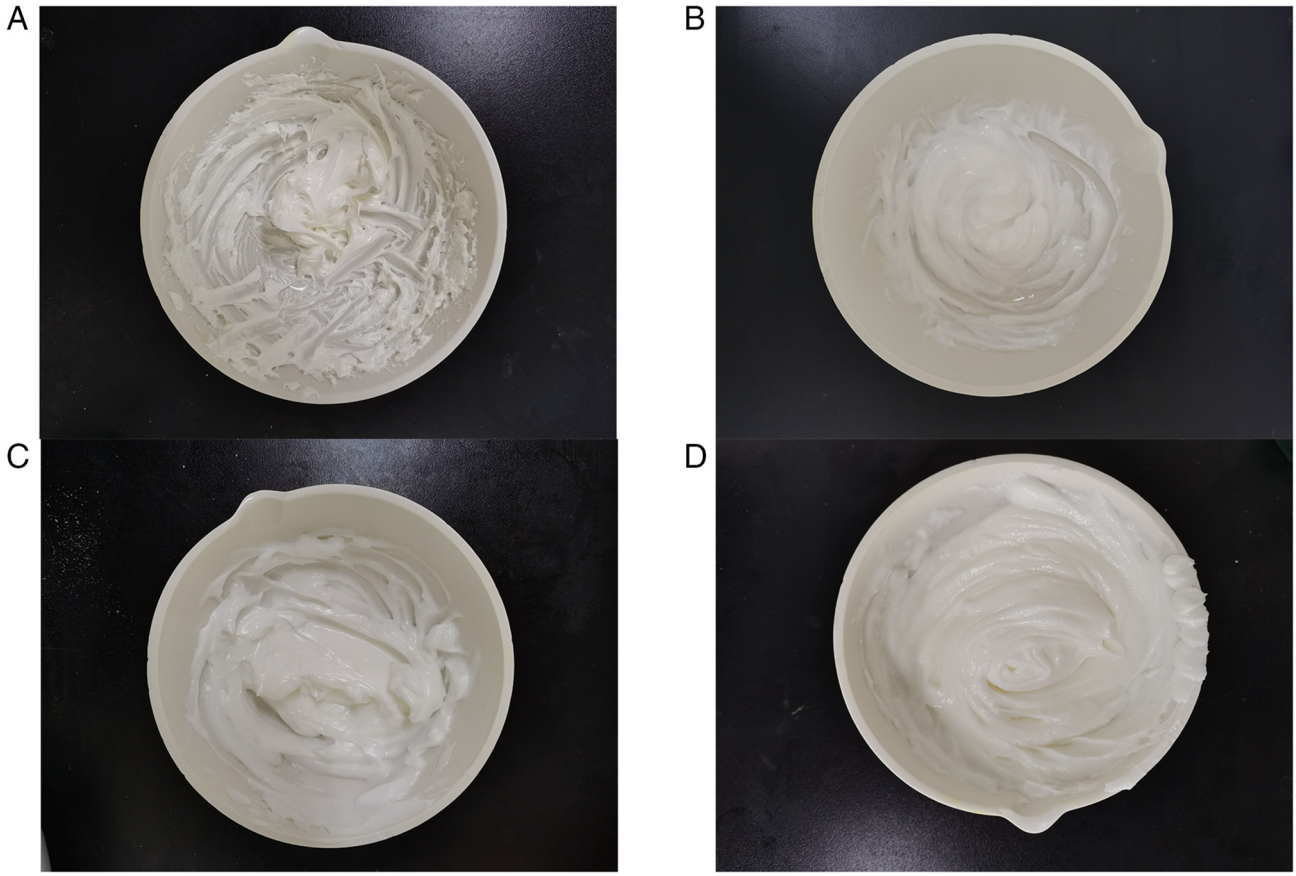

Figure 5. Appearance of the cream. (A) Prescription 1; (B) Prescription 2; (C) Prescription 3; (D) Prescription 4

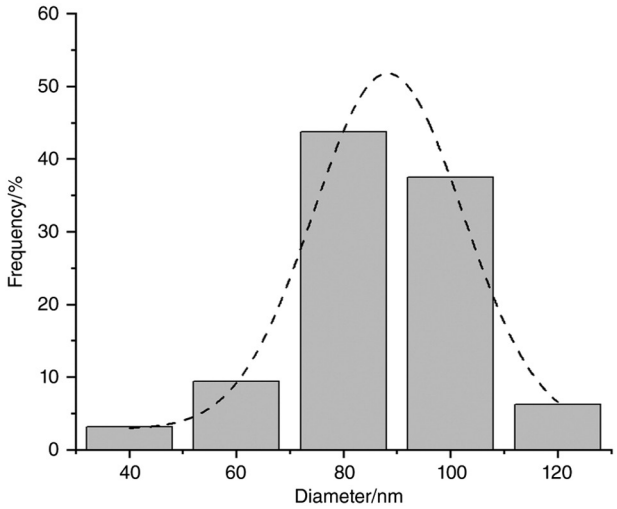

Figure 6. Particle size of drug-loaded ointment.

As shown in Fig. 15, STAT3 expression appeared as a brownish-yellow cytoplasmic staining. In the normal group, STAT3 signaling was minimal, presenting as a pale yellow hue throughout the cytoplasm. Compared with the normal group, the model group exhibited positive STAT3 expression, with deepened cytoplasmic staining in epidermal spinous layer cells and dark brown nuclei in the dermis and epidermis. Compared with the model group, the positive control group and the low-, medium- and high-dose groups of CMVO ointment exhibited lighter staining in the epidermal spinous layer, disappearance of dark brown nuclei and weaker positive STAT3 signaling expression.

Discussion

Eczema, a prevalent inflammatory skin disorder, is characterized by multiple lesions, polymorphic manifestations and intense itching (2). Environmental stimuli trigger local and systemic immune responses via the skin's neuro-immune-endocrine system, leading to various pathological changes on the skin surface (6). This condition often causes significant physical discomfort and psychological distress. While traditional topical corticosteroids are effective and widely used, their hormonal nature is associated with notable adverse effects (12,13). CMVO was selected for the present study for its anti-inflammatory and antipruritic properties, aimed at alleviating eczema symptoms (25). The first phase of this research focused on analyzing the chemical composition of *Cnidium monnieri* essential oil using GC-MS technology, identifying 21 volatile components, including isopropyl isobutyrate, (-)-β-pinene, caryophyllene, D-limonene, borneol and isobornyl acetate. Among these constituents, (-)-β-pinene, β-caryophyllene and cnidicin are known for their anti-inflammatory and antibacterial activities and are likely key contributors to CMVO's anti-inflammatory efficacy (18,19,21-23). The second phase focused on screening and optimizing the formulation of CMVO ointment by

Table XV. Quality evaluation results of different doses of *Cnidium monnieri* volatile oil cream.

Drug Content	Particle size (nm)	pH	Viscosity (mPa·S)
Low-dose group	94.50±16.88	6.92±0.00	50,553
Medium-dose group	77.77±14.92	6.91±0.02	50,533
High-dose group	84.80±6.87	6.91±0.01	49,955

Table XVI. EASI score (n=10).

Group	Day 4	Day 7	Day 10	Day 13	Day 16
Normal	0.00±0.00	0.00±0.00	0.00±0.00	0.00±0.00	0.00±0.00
Model	2.94±0.13	4.98±0.68	6.08±0.28	4.88±0.32	3.44±0.34
Positive	2.82±0.20	5.12±0.55	3.80±0.92	2.20±0.88	1.69±0.51
Low (2%)	2.91±0.12	5.61±0.42	4.43±0.46	2.87±0.73	2.21±0.72
Medium (4%)	2.98±0.15	5.32±0.62	4.14±0.56	2.56±0.47	1.76±0.46
High (8%)	3.09±0.16	5.44±0.16	4.07±0.80	2.79±0.45	1.91±0.45

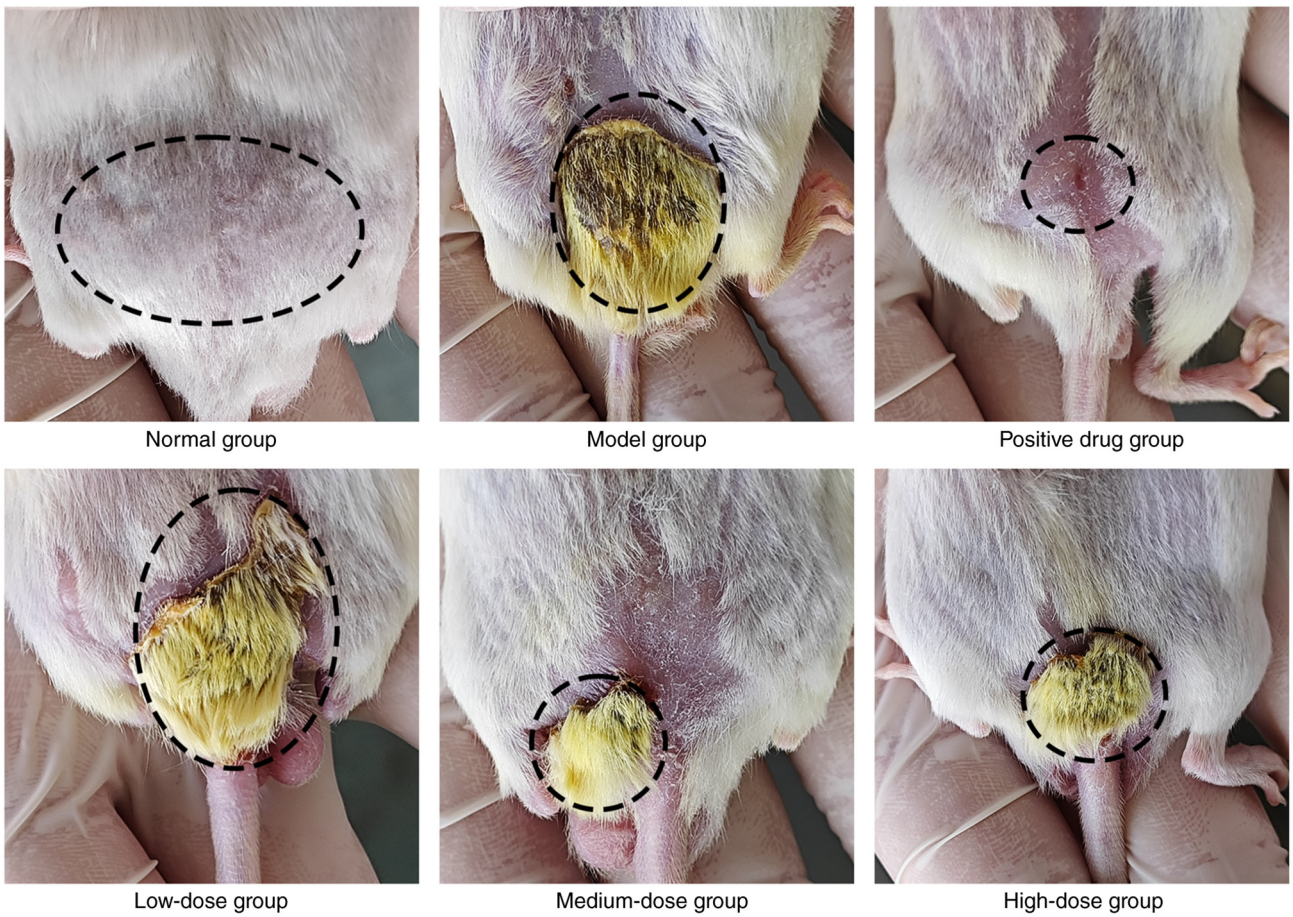

Figure 7. Observation on Day 13 of topical application to mouse skin. The ringted sections in the image indicate the normal or pathological range of the mouse's dorsal skin.

evaluating its appearance, physical stability, moisturizing properties, particle size and other characteristics. The selected cream base consists of cetyl alcohol, petrolatum, liquid paraffin, IPM, sodium lauryl sulfate, glycerin, ethyl nipagin and distilled water. Among these, cetyl alcohol acts as a thickener to enhance cream stability; petrolatum and liquid paraffin act as lubricants to regulate cream greasiness and improve spreadability; IPM functions as a penetration enhancer to

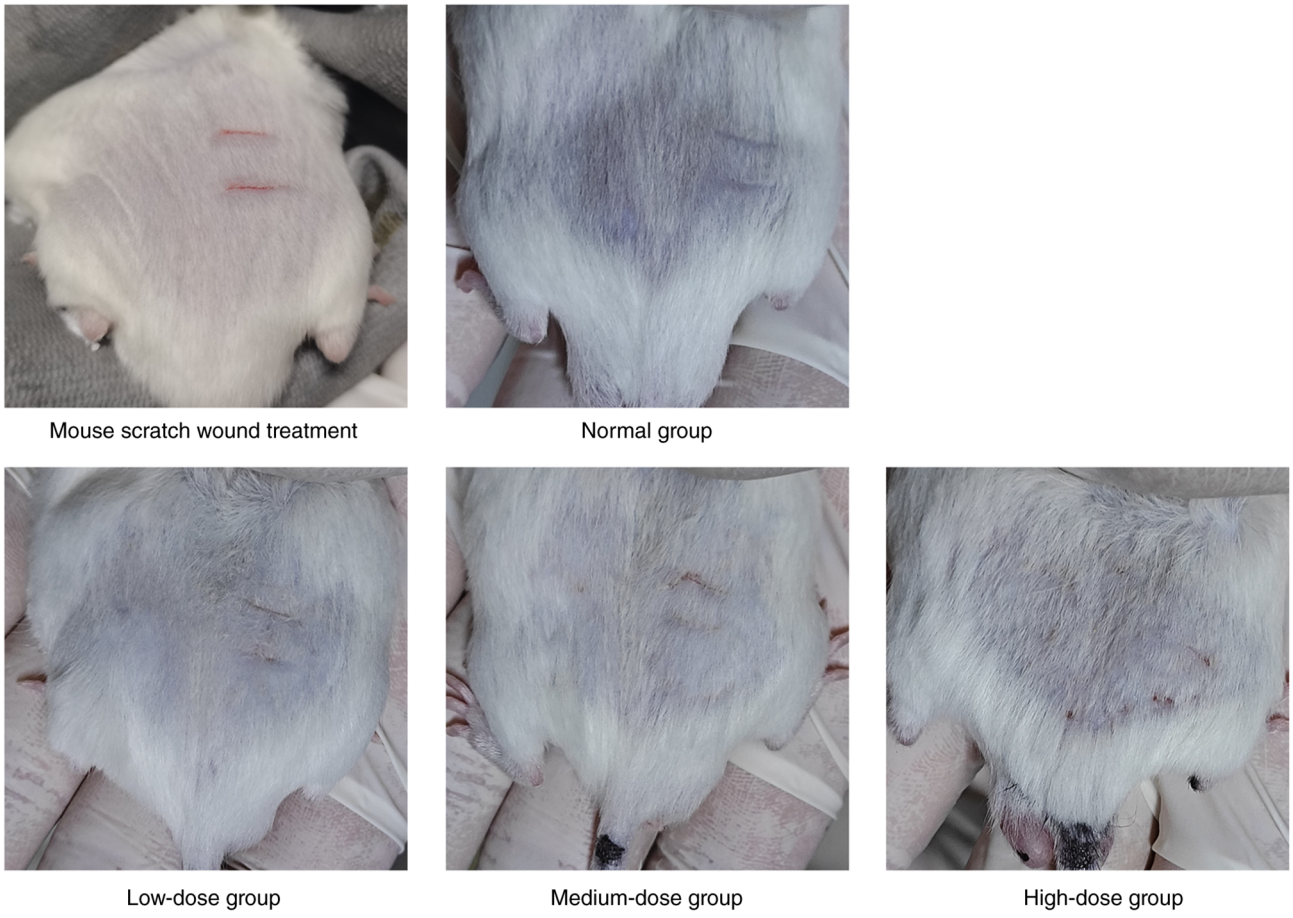

Figure 8. Observation of wound treatment on the back of mice and on the second day after drug cessation.

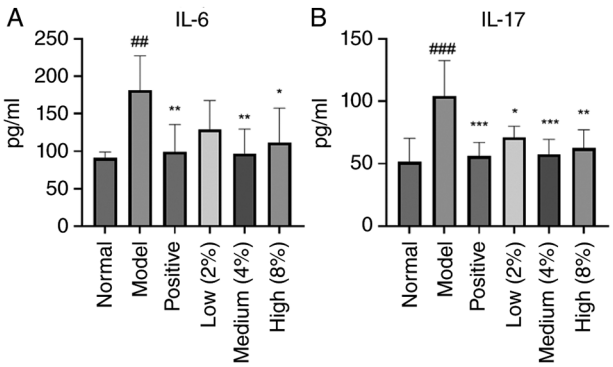

Figure 9. Expression of (A) IL-6 and (B) IL-17 in mouse serum. ##P<0.01, ###P<0.001 vs. the normal group; *P<0.05, **P<0.01, ***P<0.001 vs. the model group.

improve skin affinity; sodium lauryl sulfate acts as a surfactant to ensure emulsification between the oil and water phases; glycerin serves as a humectant, maintaining skin hydration while preventing moisture loss during storage; and propylene glycol ethyl ether functions as a preservative to ensure shelf stability. By combining these base characteristics, the fine texture exhibits excellent stability, strong moisturizing properties and easy application. To further optimize the formulation ratios, a single-factor experiment identified cetyl alcohol, IPM and sodium lauryl sulfate as the most influential factors. A response surface experiment was then conducted to determine the optimal formulation. The composition comprises: octadecanol (4.45 g), petrolatum (4 g), liquid paraffin (2.20 g), IPM (0.81 g), CMVO (1.60 g), sodium lauryl sulfate (0.39 g), glycerin (1.16 g), ethyl nicotinate (0.04 g) and distilled water (25.35 g).

The volatile oil extracted from *C. monnieri* contains components such as β-caryophyllene and cnidicin, which alleviate eczema-related itching and inflammation by inhibiting inflammatory mediators (19,23). Therefore, The present study further investigated the pharmacodynamic effects of CMVO ointment using mouse models of inflammatory responses and multiple analytical methods. The DNCB-induced eczema model in mice revealed severe lesions and erythema in the model group. Microscopic analysis showed epidermal acanthosis, dermal intercellular edema and inflammatory cell infiltration. By contrast, the positive control group treated with compound dexamethasone acetate and the low-, medium- and high-dose groups administered CMVOC showed reduced dorsal skin damage, with slight improvements in skin condition correlating with increasing CMVOC dosage. Microscopic examination further revealed a thinner stratum spinosum and fewer inflammatory cells. ELISA assays detected upregulated pro-inflammatory cytokines IL-6 and IL-17 in the model group and downregulated levels in the treatment groups, confirming CMVOC's effectiveness in suppressing eczema-related inflammatory responses.

Table XVII. Results of the irritation test.

Group/Time	Day 1	Day 2	Day 3	Day 4	Day 5	Day 6	Day 7	Day 8	Day 9	Day 10	Day 11	Day 12	Day 13	Day 14	Average points	Overall rating
Normal control skin group	0	0	0	0	0	0	0	0	0	0	0	0	0	0	0	Non-irritating
Normal control damaged group	0	0	0	0	0	0	0	0	0	0	0	0	0	0	0	Non-irritating
Low-dose treatment normal group	0	0	0	0	0	0	0	0	0	0	0	0	0	0	0	Non-irritating
Low-dose treatment damaged group	0	0	0	0	0	0	0	0	0	0	0	0	0	0	0	Non-irritating
Medium-dose treatment normal group	0	0	0	0	0	0	0	0	0	0	0	0	0	0	0	Non-irritating
Medium-dose treatment damaged group	0	0	0	0	0	0	0	0	0	0	0	0	0	0	0	Non-irritating
High-dose treatment normal group	0	0	0	0	0	0	0	0	0	0	0	0	0	0	0.04	Non-irritating
High-dose treatment damaged group	0	0	0	0	0	0	0	0	0	0	0	0	0	0	0.26	Non-irritating

Recent research on inflammatory skin diseases such as eczema has expanded such as due to their complex and diverse underlying mechanisms. Natural products have been widely studied, yielding notable progress. For instance, baicalin from *Scutellaria baicalensis* root modulates anti-inflammatory and immune responses by reducing the phosphorylation levels of JAK1, STAT1, STAT2, STAT3, STAT5 and STAT6. Essential oils from citrus plants inhibit inflammatory mediators such as IL-1β, IL-6, IL-8 and TNF-α by reducing the phosphorylation levels of STAT1 and STAT3 in the JAK-STAT pathway, as well as P-38, ERK and IKB-α in the MAPK pathway (47). Extracts from *Ginkgo biloba* leaves suppress JAK2 and STAT3 signaling-related neurotransmitters and inflammatory mediators to control itching and inflammation (48). Tripterygin such as downregulates inflammatory factors such as IL-4, TNF-α, IgE, IL-17 and IL-6, upregulates SOCS1 expression, inhibits JAK-STAT3 pathway activation, blocks T lymphocyte activation and improves inflammatory responses (49). Due to the well-established role of the JAK2-STAT3 signaling pathway in inflammatory skin diseases (50,51), this pathway was chosen for the mechanism study. In addition, key inflammatory mediators evaluated in the present study are closely associated with STAT3 signaling, supporting the relevance of this pathway.

Based on the findings from the aforementioned experiments and given that IL-17 induces increased IL-6 production, which in turn activates the JAK-STAT pathway (42) and preliminary results from H&E staining, toluidine blue staining and immunohistochemistry, CMVOC may inhibit the expression levels of JAK2 and STAT3 signaling, thereby suppressing the inflammatory response in eczema.

In the present study, a formulation of CMVO ointment was developed and optimized and the formulation underwent systematic response surface method optimization, demonstrating that the CMVOC can such as alleviate the inflammatory response associated with eczema. The volatile oil also appears to exhibit analgesic and antipruritic effects, though these were not thoroughly investigated in this experiment and warrant comprehensive future research. However, in the pharmacodynamic experiments, several serum samples in the control group were affected by hemolysis due to technical factors during blood collection. As a result, all serum-based analyses were conducted using 36 mice (n=6 per group). The reduced sample size may limit the statistical power of the present study and should be taken into consideration when interpreting the results. Nevertheless, consistent trends were observed across multiple pathological and biochemical indicators and statistically significant differences were detected between groups, which support the observed effects. Future studies with larger sample sizes are warranted to further validate and strengthen the conclusions of the present study. Furthermore, the stability of the main anti-inflammatory active substances of β-caryophyllene and cnidicin inferred from the GC-MS results can be explored in greater depth using methods such as HPLC and TLC in future research. In addition, a more comprehensive quantitative analysis of major active components would further improve the quality control of the formulation. At the same time, long-term stability and microbial stability studies are currently

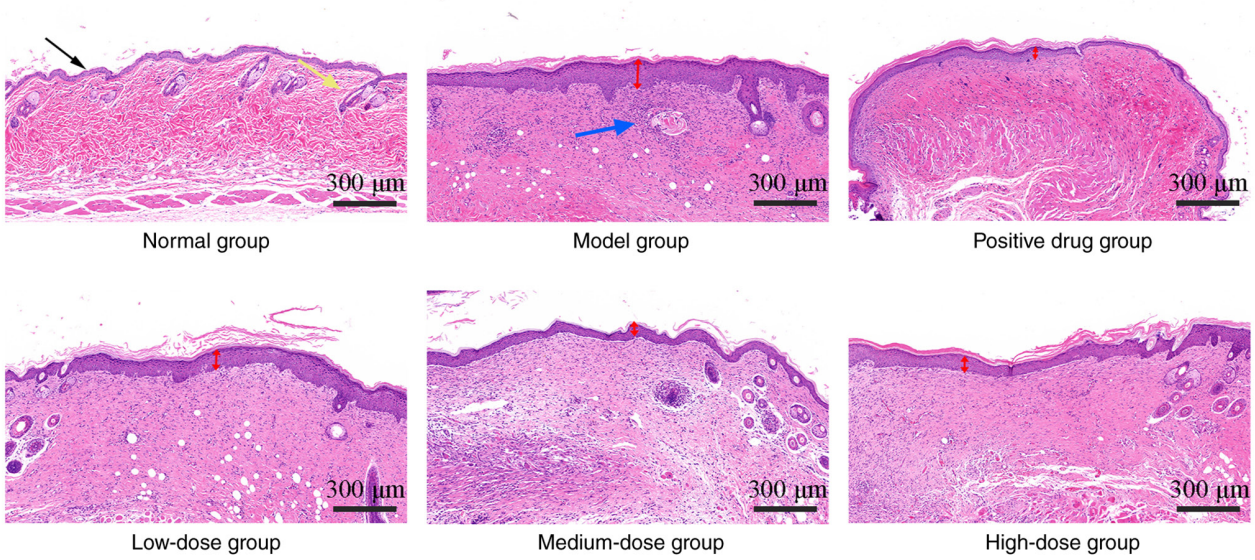

Figure 10. Hematoxylin and eosin-stained mouse skin tissue (magnification, x200). Black arrow indicates epidermis, yellow arrow indicates hair follicle, red arrow indicates granular layer and spinous layer and blue arrow indicates inflammatory cell infiltration.

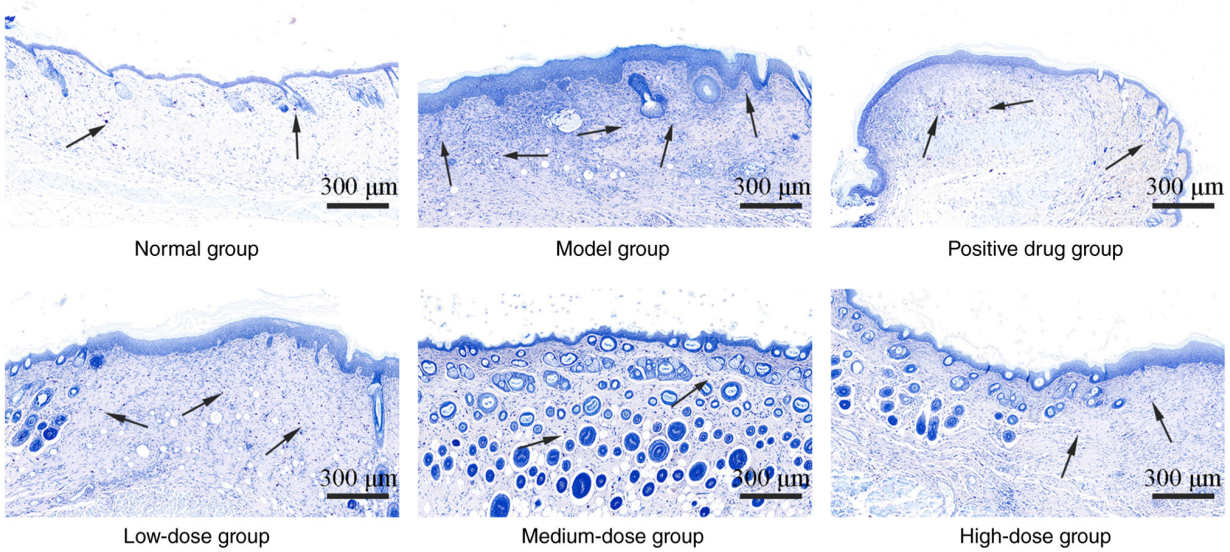

Figure 11. Toluidine blue staining of mouse skin tissue (magnification, x200). Black arrows indicate mast cells.

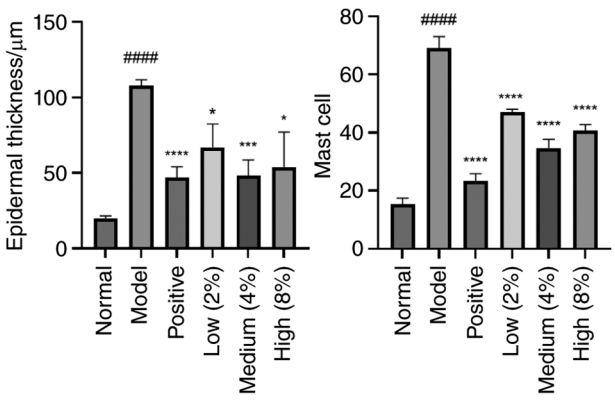

Figure 12 Epidermal thickness and mast cell count. The thickness of the epidermis was analyzed using Welch's ANOVA and the number of mast cells was analyzed using ANOVA. ####P<0.0001 vs. the normal group; *P<0.05, ***P<0.001, ****P<0.0001 vs. the model group.

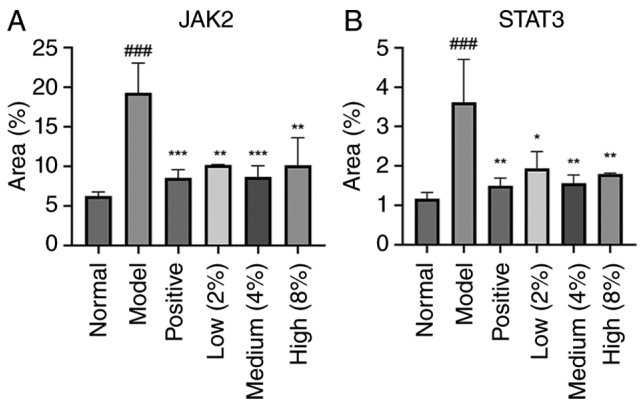

Figure 13 Effects of CMVOC on (A) JAK2 and (B) STAT3 expression in eczema-affected mice (ANOVA). ###P<0.001 vs. the normal group; *P<0.05, **P<0.01, ***P<0.001 vs. the model group. CMVOC, *Cnidium monnieri* volatile oil cream.

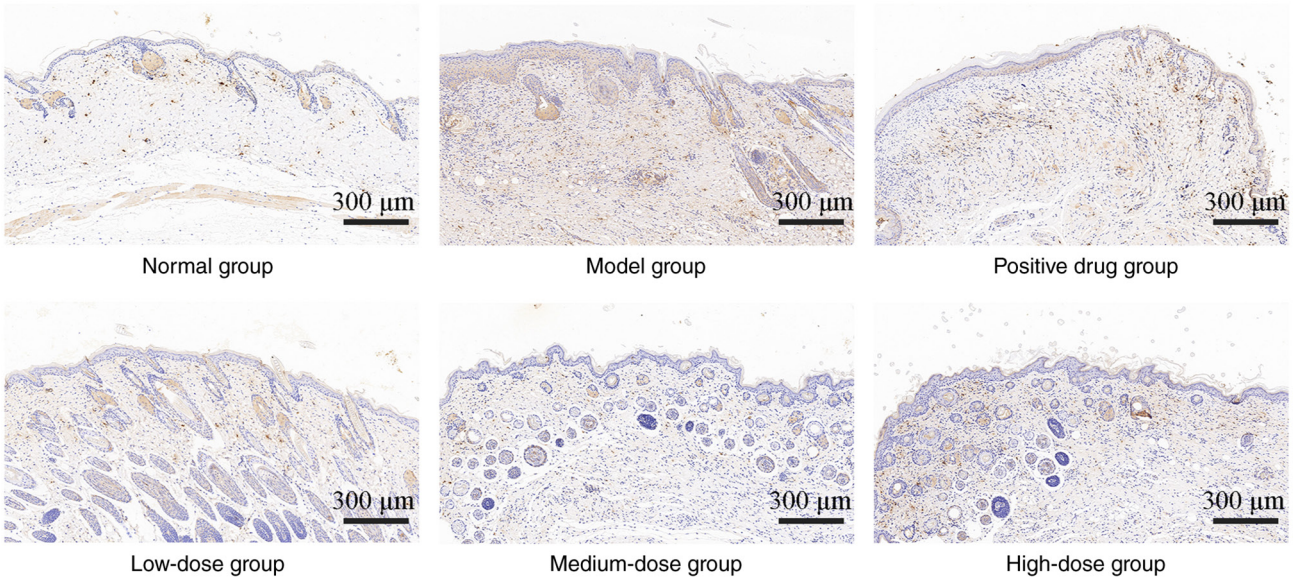

Figure 14. JAK2 signaling expression in mouse skin tissue (magnification, x200)

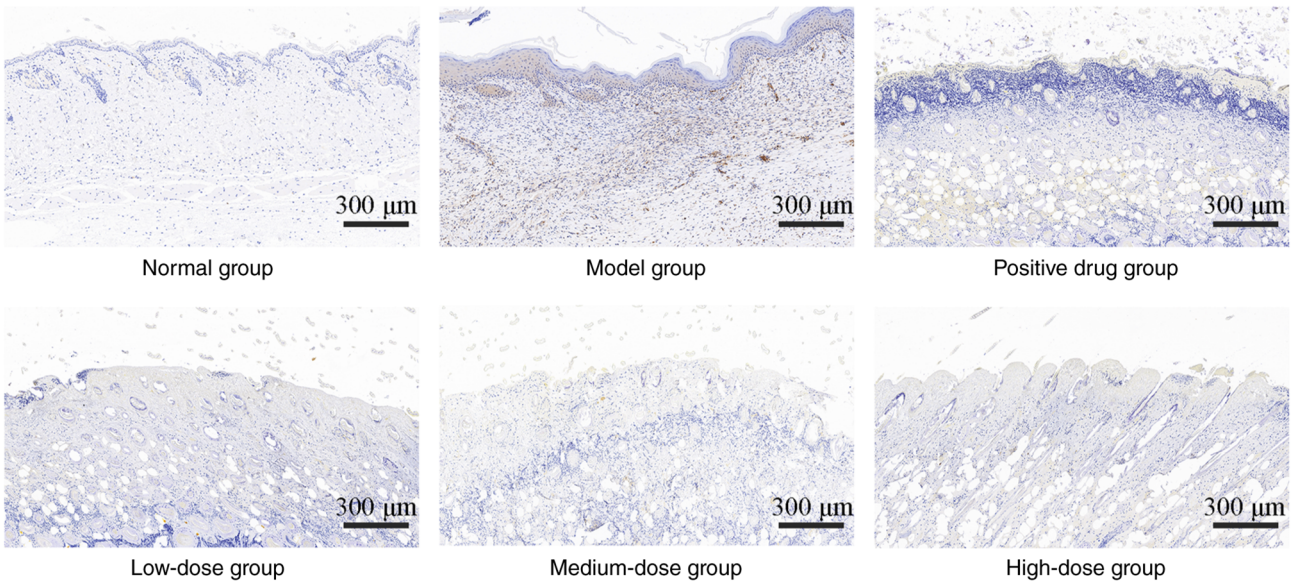

Figure 15. STAT3 signaling expression in mouse skin tissue (magnification, x200).

underway and will be reported in future work. To date, research on CMVOC has focused on pharmacodynamic evaluation, with no pharmacokinetic studies conducted yet.

However, the present study has several limitations. First, the phosphorylation levels of JAK2 and STAT3, which are critical indicators of pathway activation, were not evaluated. The current analysis was limited to total protein expression assessed by immunohistochemistry, which does not directly reflect the activation state of the JAK2/STAT3 signaling pathway. Second, pathway-specific intervention experiments (such as the use of JAK2 agonists/inhibitors or gene overexpression approaches) were not performed. Therefore, a direct causal relationship between the inhibition of JAK2-STAT3 signaling and the anti-inflammatory effects of CMVOC cannot be definitively established. Last, other inflammation-related signaling pathways, such as MAPK and NF-κB, were not investigated and their potential contributions cannot be excluded. Future investigations will focus on conducting pathway intervention experiments through pharmacological regulation, expanding the investigation to additional signaling pathways, elucidating the underlying mechanisms of action, strengthen the theoretical basis for the cream's efficacy in alleviating eczema inflammation and validating the signaling mechanism through mRNA expression analysis, western blotting analysis of phosphorylated (p-)JAK2 and p-STAT3 proteins or exploration of other signaling pathways or inflammatory factors. Clarifying relevant dose-response and time-response relationships and optimizing the administration regimen are also essential. Clinical trials are needed to confirm the safety and efficacy of treating human eczema. While the anti-inflammatory effects of CMVOC in eczema have been preliminarily demonstrated, the ointment

formulation technology remains amenable to further refinement. Additionally, combination studies with other medicinal herbs, such as *Sophora flavescens* and *Kochia scoparia*, could enhance eczema therapeutic efficacy and support the development of improved treatments.

In conclusion, the present study demonstrated that CMVOC is a safe and effective treatment for eczema, with consistent quality and notable efficacy in alleviating eczema inflammatory symptoms. These findings support further research and development, positioning CMVOC as a promising novel therapeutic option. However, clinical studies are required to validate its efficacy and optimize its therapeutic use in humans.

Acknowledgements

Not applicable.

Funding

The present study was supported by Shaanxi Provincial Department of Education Youth Innovation Team Scientific Research Plan Project (grant no. 25JP047); Shaanxi Provincial Key Research and Development Program Project (grant no. 2024CY-JJQ-36); Shaanxi Provincial Traditional Chinese Medicine Science and Technology Innovation Team (grant no. TZKN-CXTD-03); Shaanxi Provincial Department of Science and Technology Project (grant nos. 2024ZC-YYDP-110 and 2025JC-YBMS-1056); Shaanxi Province Xianyang City Science and Technology Project (grant no. L2024-QCY-ZYYJJQ-X28); Shaanxi Provincial Administration of Traditional Chinese Medicine (grant no. ZYJXG-Y23005); Key Technological Innovation Team for Industrialization of Aromatic Traditional Chinese Medicine; Shaanxi Provincial Engineering Research Center for Traditional Chinese Medicine Aromatic Industry; Key Discipline of High Level Traditional Chinese Medicine in Shaanxi Province, Traditional Chinese Medicine Processing; Shaanxi Provincial Department of Education Project (grant no. 24JP045); Innovation and Entrepreneurship Training Program for College Students (grant no. S202410716081). Youth Innovation Team of Shaanxi Universities for Traditional Chinese Medicine Health-Care Technologies in Elderly Chronic Disease Management; Qin Chuangyuan Project for Innovation and Agglomeration of Traditional Chinese Medicine Industry (grant no. L2024-QCY-ZYYJJQ-X69).

Availability of data and materials

The data generated in the present study are included in the figures and/or tables of this article.

Authors' contributions

Experimental designer was TS. Experimental procedures were performed by TS, LD, BZ, XD and XG. Result analysis was by TS, JieW and JinW. TS drafted the initial manuscript. YW, XZ and TS confirm the authenticity of all the raw data. HN, JS, YS, DG, JZ and XS conducted data analysis and confirmed the results. Manuscript revision and editing was by XZ, XS, YW, HN, JS, YS, DG and JZ. YW proposed the research direction of the present study, supervised the implementation of experiments, revised the manuscript and addressed the comments raised by the reviewers. All authors read and approved the final manuscript.

Ethics approval and consent to participate

The animal studies were reviewed and approved by the Laboratory Animal Welfare Ethics Committee, which was approved by Shaanxi University of Chinese Medicine (approval no. SUCMDL20250512001). ARRIVE guidelines were followed.

Patient consent for publication

Not applicable.

Competing interests

The authors declare that they have no competing interests.

References

1. Chovatiya R: Atopic dermatitis (eczema). JAMA 329: 268, 2023.
2. Tokura Y, Yunoki M, Kondo S and Otsuka M: What is 'eczema'? J Dermatol 52: 192-203, 2025.
3. Schmitt J, Apfelbacher CJ and Flohr C: Eczema. BMJ Clin Evid 2011: 1716, 2011.
4. Liu Y, Sun S, Zhang D, Li W, Duan Z and Lu S: Effects of residential environment and lifestyle on atopic eczema among preschool children in Shenzhen, China. Front Public Health 10: 844832, 2022.
5. Long Q, Jin H, You X, Liu Y, Teng Z, Chen Y, Zhu Y and Zeng Y: Eczema is a shared risk factor for anxiety and depression: A meta-analysis and systematic review. PLoS One 17: e0263334, 2022.
6. Slominski RM, Raman C, Jetten AM and Slominski AT: Neuro-immuno-endocrinology of the skin: How environment regulates body homeostasis. Nat Rev Endocrinol 21: 495-509, 2025.
7. de Lusignan S, Alexander H, Broderick C, Dennis J, McGovern A, Feeney C and Flohr C: The epidemiology of eczema in children and adults in England: A population-based study using primary care data. Clin Exp Allergy 51: 471-482, 2021.
8. Zhang J, Zhu S, Yuan L, Yu X, Ling S, Zhang J and Yang B: Assessing atopic dermatitis control in Chinese patients: Validation of the chinese version of recap of atopic eczema questionnaire (RECAP) and an investigation into its interpretability. Acta Derm Venereol 105: adv43458, 2025.
9. Ferreira MA, Vonk JM, Baurecht H, Marenholz I, Tian C, Hoffman JD, Helmer Q, Tillander A, Ullemar V, van Dongen J, *et al*: Shared genetic origin of asthma, hay fever and eczema elucidates allergic disease biology. Nat Genet 49: 1752-1757, 2017.
10. Marenholz I, Arnau-Soler A, Rosillo-Salazar OD and Lee YA: New insights from genetic studies of eczema. Med Genet 35: 33-45, 2023.
11. Lax SJ, Harvey J, Axon E, Howells L, Santer M, Ridd MJ, Lawton S, Langan S, Roberts A, Ahmed A, *et al*: Strategies for using topical corticosteroids in children and adults with eczema. Cochrane Database Syst Rev 3: CD013356, 2022.
12. Ference JD and Last AR: Choosing topical corticosteroids. Am Fam Physician 79: 135-140, 2009.
13. Stacey SK and McEleney M: Topical corticosteroids: Choice and application. Am Fam Physician 103: 337-343, 2021.
14. Sun Y, Yang AWH and Lenon GB. Phytochemistry, Ethnopharmacology, Pharmacokinetics and Toxicology of *Cnidium monnieri* (L.) Cusson. Int J Mol Sci 21: 1006, 2020.
15. Yuan S, Liu M, Duan X and Zheng Y: Research progress on the processing history, chemical constituents and pharmacological effects of cnidii fructus. Chin Wild Plant Resour 42: 74-81, 2023.

16. Arizmendi N, Alam SB, Azyat K, Makeiff D, Befus AD and Kulka M: The complexity of sesquiterpene chemistry dictates its pleiotropic biologic effects on inflammation. Molecules 27: 2450, 2022.
17. Paço A, Brás T, Santos JO, Sampaio P, Gomes AC and Duarte MF: Anti-inflammatory and immunoregulatory action of sesquiterpene lactones. Molecules 27: 1142, 2022
18. Ahn SS, Yeo H, Jung E, Ou S, Lee YH, Lim Y and Shin SY: β-Caryophyllene ameliorates 2,4-dinitrochlorobenzene-induced atopic dermatitis through the downregulation of mitogen-activated protein kinase/EGR1/TSLP signaling axis. Int J Mol Sci 23: 14861, 2022.
19. Scandiffio R, Geddo F, Cottone E, Querio G, Antoniotti S, Gallo MP, Maffei ME and Bovolin P: Protective effects of (E)-β-caryophyllene (BCP) in chronic inflammation. Nutrients 12: 3273, 2020.
20. Kotan R, Kordali S and Cakir A: Screening of antibacterial activities of twenty-one oxygenated monoterpenes. Z Naturforsch C J Biosci 62: 507-513, 2007.
21. Salehi B, Upadhyay S, Erdogan Orhan I, Kumar Jugran A, L D Jayaweera S, A Dias D, Sharopov F, Taheri Y, Martins N, Baghalpour N, *et al*: Therapeutic potential of α- and β-pinene: A miracle gift of nature. Biomolecules 9: 738, 2019.
22. Sun M, Sun M and Zhang J: Osthole: An overview of its sources, biological activities, and modification development. Med Chem Res 30: 1767-1794, 2021.
23. He S, Liang X, Chen W, Nima Y, Li Y, Gu Z, Lai S, Zhong F, Qiu C, Mo Y, *et al*: Osthole ameliorates chronic pruritus in 2,4-dichloronitrobenzene-induced atopic dermatitis by inhibiting IL-31 production. Chin Herb Med 17: 368-379, 2024.
24. Feng X: Research progress on the applicability of essential oils in promoting permeation. Chin Tradit Pat Med 35: 157-161, 164, 2013 (In Chinese). https://qikan.cqvip.com/Qikan/Article/Detail?id=44468738.
25. Wang XD, Bai JL, Ma ZJ, Fan J, Kong WB, Wang JL, Zhang J and Liang JY. Analysis of chemical composition, antibacterial activity, antioxidant properties, and cytotoxicity of essential oils from four plant fruits. Microb Pathog 209: 108133, 2025.
26. Sattayakhom A, Wichit S and Koomhin P: The effects of essential oils on the nervous system: A scoping review. Molecules 28: 3771, 2023.
27. Sharmeen JB, Mahomoodally FM, Zengin G and Maggi F: Essential oils as natural sources of fragrance compounds for cosmetics and cosmeceuticals. Molecules 26: 666, 2021.
28. Zhang X, Huang J, Xie Z, Chen F, Chen H, Liao Y, Xu J and Yue P: Research progress on stabilization techniques of volatile oils from traditional Chinese medicine and their preparations application. Chin Herb Drugs 56: 5258-5266, 2025.
29. Sawant A, Kamath S, Kg H and Kulyadi GP: Solid-in-oil-in-water emulsion: An innovative paradigm to improve drug stability and biological activity. AAPS PharmSciTech 22: 199, 2021.
30. Li C: Study on preparation technology and quality standard of Longzi Xiaozhong Cream (unpublished thesis). Yunnan University of Chinese Medicine, 2023.
31. Ji X, Li X, Yang R, Zhao H, Zhai X, Ji L and Yang L: Study on preparation of Aijiaohuang Cream and improvement of psoriasis mice skin lesions. Shizhen Guoyi Guoyao 35: 625-628, 2024 (In Chinese). https://doi.org/10.3969/j.issn.1008-0805.2024.03.26.
32. He L, Li H, Li W, Li C and Zhang J: Preparation technology of anti-inflammatory acne cream. J Shanxi Med 51: 2171-2175, 2022 (In Chinese). https://qikan.cqvip.com/Qikan/Article/Detail?id=7108662780.
33. Yang J, Wang J, Wang L, Dong Y and Li X: Study on insect-proof cream based on plant essential oil. Guangzhou Chem Ind 51: 37-39, 2023 (In Chinese). https://qikan.cqvip.com/Qikan/Article/Detail?id=7110941216.
34. Liu H, Cai Y, Chu Y, Yu X, Song F, Wang H, Zhang H and Sun X: Formulation of chrysomycin A cream for the treatment of skin infections. Molecules 27: 4613, 2022.
35. Salehi N, Mortazavi SM and Moghimi H: Investigating the changes in cream properties following topical application and their influence on the product efficiency. Iran J Pharm Res 21: e123946, 2022.
36. Liao J, Lei Y, Chen J, Wei D, Zhou B, Liang J, Su R, Chen G: Optimization of forming process of Zhuangfang Xiaoji Yeti Cream by Box-Behnken response surface methodology. J China Prescr Drug 23: 16-20, 2025 (In Chinese). https://qikan.cqvip.com/Qikan/Article/Detail?id=7201293506.
37. Duan J, Li J, Wang Y, Zhoua P, Wanga X, Xiaa N, Wanga J, Lia J, Wang W, Wang X, *et al*: Therapeutic effects and mechanism of action of lavender essential oil on atopic dermatitis by modulating the STAT3/RORγt pathway. Arab J Chem 17: 105525, 2023.
38. Matsuki F, Suzuki S, Hirose T, Suzuki T, Yoshida T, Onishi Y and Yamamoto R: Prescription and application adequacy of topical corticosteroids based on the finger-tip unit method in adult patients with atopic dermatitis: A cross-sectional study. J Gen Fam Med 26: 547-554, 2025.
39. Bakó E, Fehérvári P, Garami A, Dembrovszky F, Gunther EE, Hegyi P, Csupor D and Böszörményi A: Efficacy of topical essential oils in musculoskeletal disorders: Systematic review and meta-analysis of randomized controlled trials. Pharmaceuticals (Basel) 16: 144, 2023.
40. Yang W: Study on the efficiency and safety of Co-glycyrrhetinic acid cream (unpublished thesis). Hebei Medical University, 2015.
41. Hanifin JM, Baghoomian W, Grinich E, Leshem YA, Jacobson M and Simpson EL: The eczema area and severity index-A practical guide. Dermatitis 33: 187-192, 2022.
42. Cai Y, Zhao S, Yan W, Lin X, Gou W, Ye M, Wu Y and Zhang W: Preliminary research on the effect of volatile oil from *Eugenia caryophyllata* Thunb. on the skin of mice. Chinese Ethnic and Folk Medicine 32: 23-27, 2023 (In Chinese). https://qikan.cqvip.com/Qikan/Article/Detail?id=7110472857.
43. Fischer AH, Jacobson KA, Rose J and Zeller R: Hematoxylin and eosin staining of tissue and cell sections. In: Spector DL, Goldman RD (eds.). Basic Methods in Microscopy. Cold Spring Harbor Laboratory Press, Cold Spring Harbor, NY, 2006, Ch. 4.
44. Raja N, Naikodi S, Govindarajan A and Palanisamy K: Toluidine blue staining of murine mast cells and quantitation by a novel, automated image analysis method using whole slide skin images. J Histotechnol 44: 190-195, 2021.
45. Hong S, Lee B, Kim JH, Kim EY, Kim M, Kwon B, Cho HR, Sohn Y and Jung HS: Solanum nigrum Linne improves DNCB-induced atopic dermatitis-like skin disease in BALB/c mice. Mol Med Rep 22: 2878-2886, 2020.
46. Oumarou Hama H, Aboudharam G, Barbieri R, Lepidi H and Drancourt M: Immunohistochemical diagnosis of human infectious diseases: A review. Diagn Pathol 17: 17, 2022.
47. Fan X, Liu Z, Yang W, Zhang H, Zhong H, Pang Y, Ye X, Wu C and Li L: Advances in atopic dermatitis treatment: From pathogenesis to natural product-based therapies. Phytother Res 39: 4444-4473, 2025.
48. Chummun Phul I, Gómez-Llonín A and Bhaw-Luximon A: From traditional medicine to nanomedicine: Potential of *Ginkgo biloba* extracts in treating inflammatory skin diseases. RSC Med Chem 15: 2643-2656, 2024.
49. Duan Y, Zhu L and Dong Y: Protective effect and mechanism of tripterine on atopic dermatitis in mice based on SOCS1/JAK-STAT3pathway. J Guangxi Med Univ 39: 290-297, 2022.
50. Zeng H, Zhao B, Zhang D, Rui X, Hou X, Chen X, Zhang B, Yuan Y, Deng H and Ge G: Viola yedoensis Makino formula alleviates DNCB-induced atopic dermatitis by activating JAK2/STAT3 signaling pathway and promoting M2 macrophages polarization. Phytomedicine 103: 154228, 2022.
51. Wen C, Yang X, Han Y, Fu Y, Chen W, Zhang H, Zhang X, Xiao Z, Cheng G and Zhang J: Integrating network pharmacology and experimental validation to elucidate the mechanism of Xiao-bi decoction in psoriasis treatment: Inhibition of JAK2/STAT3 signaling and rebalancing Th17/Treg responses. J Ethnopharmacol 363: 121477, 2026.